Safety in Mines Research Advisory Committee

Final Project Report

DETERMINING THE FRICTION FACTORS FOR UNDERGROUND COLLIERY BORD AND PILLAR WORKINGS

C F MEYER

Research Agency: Varicon cc

Project Number: Col 465

Date of report: May 1998

Preface

This project was mainly proposed to make available, to the coal mining industry, a set of default friction values that could be used with more confidence in network simulation programs. In the past only values from the USBM and that were generally more related to metalliferous mines were available. The need was therefore identified for a number of investigations to collect data that represent the majority of the coal mining industry and in particular those mines that practice bord and pillar mining.

During the project, use was made of both underground investigations and CFD simulations to provide as much information as possible on the effect of different conditions and parameters on pressure loss and on k-factors and airflow behaviour. K-factors for a number of underground scenarios were measured and compared with data that was gathered from an extensive literature study that was performed as part of the project.

To validate and to prove the reliability of the CFD results, two underground scenarios were measured and the detail modelled on the computer. The results were compared and proved that the numerical results and the experimental results were within 10% of each other. By applying a correction factor, the CFD simulations that followed could be calibrated to be more representative of the underground conditions.

At the end of the project it is possible to provide a set of values and results that represent intake and return airways, dyke areas, aircrossings, an empty raise-bore shaft, the effect of different pillar lengths on pressure loss, the optimum position for a stopping inside a side road and the airflow behaviour through a multiple roadway situation.

Acknowledgements

Table of Contents:

4

Table of Contents (cont'd)

Table of Contents (cont'd)

List of Figures:

List of Figures (cont'd)

List of Figures (cont'd)

9

List of Figures (cont'd)

List of Tables:

List of Tables (cont'd)

1   Introduction

Throughout the years, ventilation practitioners have been using frictional resistance values for performing ventilation planning exercises and also to evaluate the current status of the ventilation districts in the mine with regard to the availability of air supply to the sections.

For these planning exercises to be accurate and the information to be useful, the friction and/or resistance values must be as accurate as possible. The difficulty starts when these friction factors are measured in the typical underground scenario by using whatever means possible, ranging from a trailing hose to handheld barometers.

A series of values are available for use in metalliferous mines as a result of numerous tests that were performed over the past number of years. These results are not suitable, however, for evaluating airflow in coal mines because the mining and geological conditions and therefore the airflow behaviour are so much different from that of the metalliferous mines.

It was for this reason that this project was initiated on behalf of coal mines through the SIMRAC process. The aim was to provide the ventilation practitioner on the coal mines with a set of basic values that could be used to perform ventilation planning on coal mines with confidence and that could be related to the underground coal mine bord and pillar situation.

This document provides information that was gathered from a comprehensive literature study into the methods and procedures used locally and internationally to determine friction and resistance values. The literature study also reveals information on the theory and principles behind the concept of using frictional resistance values.

Furthermore this document reports on the results obtained from tests and measurements taken both during physical underground measurements and through using Computational Fluid Dynamics (CFD).

In the last section of this document, a summary of all relevant information and values will be provided for easy reference to the end user.

2 Literature Review

The literature review concentrated on work that was done in coal mines and other related areas, both in overseas and local mines.

2.1 Background information

The importance of planning ventilation systems in modern mines can hardly be over emphasised from a cost point of view. In order for correct planning the ventilation practitioner not only needs to know the laws of airflow, but also requires reliable data on the related parameters. The parameters of importance in ventilation planning are air quantity (Q), pressure (P) and resistance (R). The relationship between these parameters is presented by the following:

$$P = RQ^2$$

known in ventilation planning as the square law.

The relationship between different units and terms used and applied in ventilation were described by Holding[1] in 1970 and by McPherson[2] in 1971.

Air flowing in a mine airway contains energy in the form of static pressure and velocity pressure. The total pressure is the sum of these two components, and will theoretically remain constant. In practice, however, the total pressure does not remain constant but is reduced, due to friction and shock.

One of the duties of the ventilation practitioner is to conduct ventilation surveys. These surveys are conducted to establish the resistance of the mine airways. The resistance of an airway or a system can be defined as the relationship between the pressure loss along the airway or through the system and the quantity of air flowing along the airway or through the system. The resistance values obtained are then used in the planning of the ventilation needs for the future development of the mine. The resistance includes the effects of bends, equipment in airways, and the causes of shock losses. In the planning for the future development of a mine, physical measurements cannot be taken and therefore empirical factors need to be calculated based on a knowledge of conditions prevailing in a mine. The resistance is then given by the following relationship:

$$R = \frac{KLO}{A^3} \qquad (1)$$

with $K =$ friction factor (Ns^2/m^4)

$L =$ length of airway (m)

$O =$ airway perimeter (m)

$A =$ cross-sectional area (m^2)

To empirically determine the resistance, an analogy can be drawn between the air flowing in the mine and the resistance to flow of a fluid in a pipe. In a pipe, a combination of the following factors contributes to resistance:

♦ Internal friction, viscosity of the fluid.

♦ Friction between the pipe and the fluid.

♦ Changes in the area and the direction of flow.

♦ Obstructions in the flow path.

The first two factors can be classified as friction losses and constitute about 70 % of the pressure loss in mine ventilation. The last two factors account for 30 % of the pressure loss and are seen as shock losses. Both of these two, friction losses and shock losses, must be taken into consideration when designing the ventilation requirements of a mine, as they constitute the components responsible for energy losses due to air flow through mine openings.

2.2 Friction factor

The friction factor, K, which is used in estimating roadway resistance and ventilation pressure, plays an important part in determining the energy losses in the process of planning a ventilation system. The actual K - factor is site dependent and depends on the following:

♦ Mining method

♦ Airway parameters

♦ Type of entry

♦ Roof support system

2.2.1 Theory

As air is a fluid[1] the general theories of fluid mechanics can be applied to the flow of air in a mine, similar to the flow of water in a pipe. The Darcy - Weisbach equation:

$$h_f = \frac{fLV^2}{2Dg} \qquad (2)$$

with:

h_f – head loss [m]

L – length of pipe [m]

V – fluid mean velocity [m / s]

D – diameter of pipe [m]

g – gravitational acceleration [m / s^2]

f – dimentionless friction coefficient

is applicable to head loss calculations in both laminar and turbulent conditions. The formula was derived for use in circular cross sections. It can, however, be used for any shape with the following modification D = 4A/P (A = cross section area of the airway, P = wetted perimeter of the airway). This equation (1) relates the physical parameters of the conduit and fluid velocity to the energy that is needed to create flow. The influence of the wall-surface interface is represented by the Darcy friction coefficient (f), which is a function of the Reynolds Number $R_N = VD\rho/\mu$, relative roughness $\varepsilon = e/D$, roughness distribution s/D, and shape factor m. Therefore:

$$f = f(R_N, \varepsilon, s/D, m) \qquad (3)$$

Nikuradse determined the relationships in (2) experimentally for sand-roughened pipes, for which the friction coefficient is then given by:

$$f = \frac{1}{\left(1,14 + 0,86\ln\dfrac{e}{D}\right)^2} \qquad (4)$$

---

[1] **Fluid** - any liquid or gas; any substance that flows. The World Book Dictionary.

Therefore if the value of f is known for a pipe with "wholly rough" flow, and the pressure loss is proportional to the square of the velocity, the roughness height e can be calculated using:

$$e = D \exp \left(\frac{\frac{1}{1,14-0,86f}}{0,86} \right) \qquad (5)$$

Moody[3] constructed a chart for determining the friction coefficients in commercial pipes. The chart is presented in Figure 2.2.1. and expresses the relationship between friction coefficient and Reynolds number for various constant values of relative roughness. It involves only dimensionless quantities and is therefore applicable in any system of units. From the chart, if the friction factor f is larger than 0,005 and the Reynolds number exceeds 1 000 000, the friction factor becomes independent of the Reynolds number and varies with roughness e/D only.

In mine ventilation, an alternative friction factor, referred to as the Atkinson's friction factor, k, is used instead of f. Atkinson arrived at this factor by assuming that pressure loss is proportional to the airway length L, perimeter P, square of velocity V, and inversely proportional to the area A. The Atkinson's formula is given by:

$$p_f = \frac{kLP}{A} V^2 \qquad (6)$$

The equation in (5) is similar to (1) when expressed as a pressure loss due to friction. By equating these two relationships under these conditions, the relationship between f and k will be given by:

$$f = 8k \qquad (7)$$

To include the standard air density in the Atkinson's friction factor, use is made of $K = k * \rho$. To apply corrections to determine the pressure loss according to the air density the following is used:

$$K = K_s \frac{\rho}{\rho_s} \qquad (8)$$

where K_s is the Atkinson friction factor for standard air density $\rho = 1,2 \left[\frac{kg}{m^3} \right]$.

17
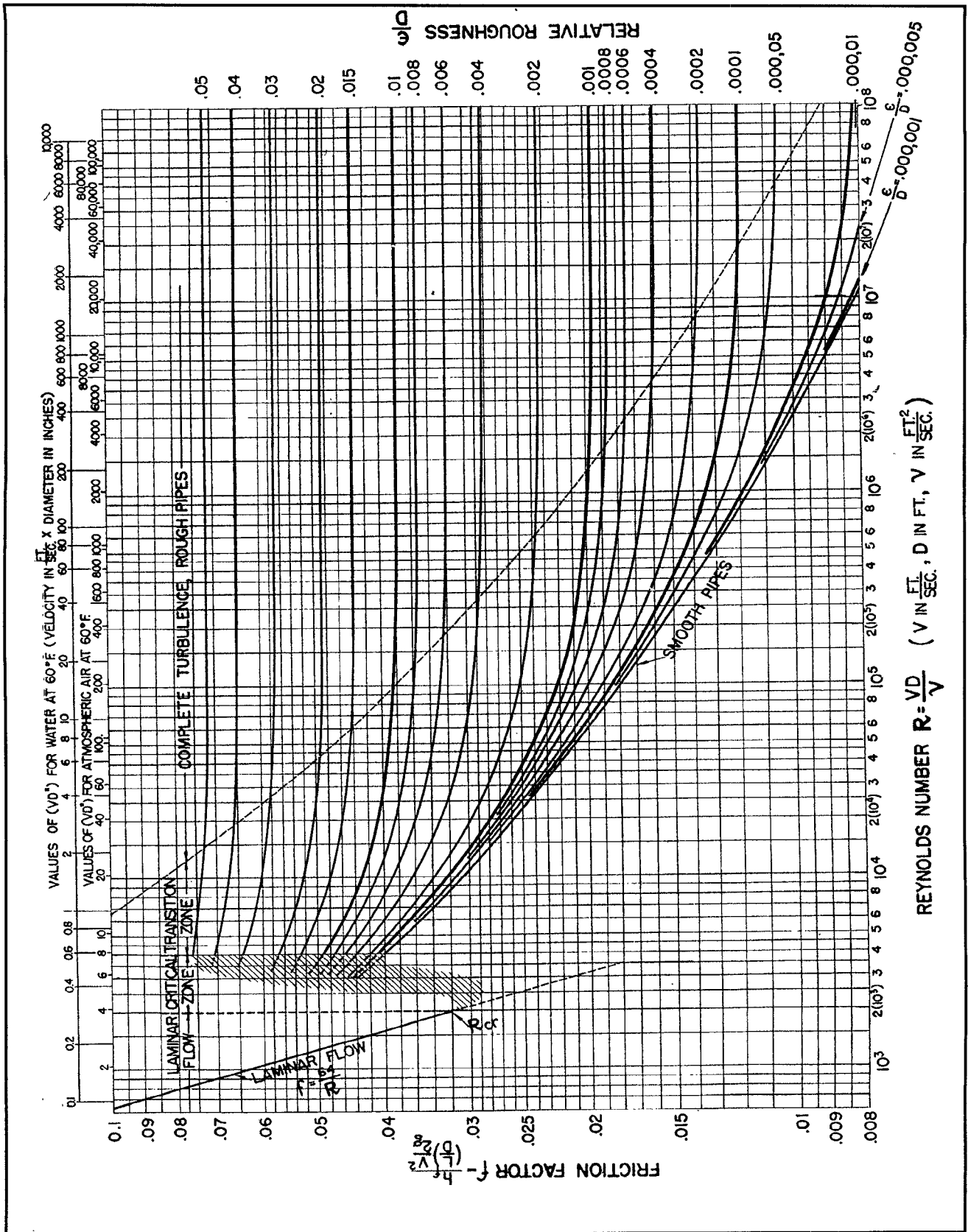
Figure 2.2.1: Moody's chart for friction coefficients in commercial pipes

18

Burrows[4] showed the relation between $\dfrac{Ns^2}{m^2}$ and $\dfrac{kg}{m^3}$ as the units for K, which is repeated below.

$$K = \frac{Ns^2}{m^2} = \left(kg\frac{m}{s^2} \right)\frac{s^2}{m^4} = \frac{kg}{m^3} \qquad (9)$$

Although the units of K and air density are the same, they are not related. The friction factor is constant and does not depend on the density of the air flowing in the airway. However, the pressure loss is directly proportional to density of the air. The K value is only dependent on the physical characteristics, such as the roughness of the airway.

2.2.2 Measurements

The flow through a mine falls into the turbulent zone; the friction coefficient, f, can thus be determined based on a knowledge of the airway geometry and assessed roughness.

Wala[5] used four types of measurements to determine the K-factor. These measurements were:

a) **Pressure loss across the tested airways.** Two methods were used to determine the pressure losses. The first method made use of plastic tubes and a sensitive pressure gauge. The difference in total pressure, between two points, was directly measured. For the second method sensitive electronic micro-barometers was used. In this method the absolute pressure at different points were measured.

b) **Airflow quantity.** The airflow quantity was the product of the air velocity and the cross sectional area at the point where the air velocity was measured. The air velocity measurement was done using two different methods. The first was through the use of vane anemometers, while the second utilised a hot wire anemometer.

c) **Air density.** This was determined through the measurement of dry and wet bulb temperatures and barometric pressure.

d) **Geometrical parameters.** The cross sectional area, perimeter and lengths of test sections were computed with data obtained with a tape measure.

To avoid shock effects, measurements should be confined to straight, unobstructed, clean, and relatively new airways.

Rahim[6] made use of the following instruments during his investigation:

Pressure survey meter with accessories. The pressure survey meter was calibrated to directly read the pressure differences. It was calibrated for an air density at $18,83°$ C, 760 mm barometric pressure and 50 per cent relative humidity.

Anemometer with extension rods, tape, stop watch. Air velocities were measured with the anemometer at least 1,2 m from the observer's body.

Whirling hygrometer. The hygrometer used was graduated from 0 to $50°$C, with an accuracy of $0,1°$ C.

Aneroid barometer. The barometer had a range of 720 mm Hg to 800 mm Hg with an accuracy of 0,5 mm Hg.

They performed the same type of measurements as Wala to obtain the information from which the value of 'K' was then determined.

Deglon and Hemp[7] conducted pressure surveys for South African bord and pillar mines in 1992. They used the training hose method, using a 6 mm diameter plastic hose, and pressure differentials were measured with an electronic digital manometer.

Martinson et al[8] reported on work that was done in a TRONA mine in Green River, Wyoming. The mining methods are similar to coal mining, i.e. drill and blast or continuous miner. The tests were carried out in a bord and pillar section where the roof support was done by roofbolting which was supplemented with lacing in highly stressed zones. Pressure differences were measured, using normal garden hose and then measuring the pressure differences between different points; at the same measuring points the flowrates were also determined.

2.2.3 Results

In 1927 McElroy and Richardson[9] did an extensive study to determine friction factors. They compiled a table of friction factors that was applied to the design of airways. A copy of their table and an SI conversion thereof are presented in Tables 2.2.3(a) and 2.2.3(b).

Table 2.2.3(a): U.S.B.M. schedule of friction factors for mine airways

| Type of airway | Irregularities of surfaces, areas, and alignment | Straight | | | Sinuous or curved | | | | | | | | |
| | | | | | Slightly | | | Moderately | | | High degree | | |
		Clean (basic values)	Slightly ob-structured	Moder-ately ob-structured	Clean	Slightly ob-structured	Moder-ately ob-structured	Clean	Slightly ob-structured	Moder-ately ob-structured	Clean	Slightly ob-structured	Moder-ately ob-structured
Smooth lined	Minimum	10	15	25	20	25	35	25	30	40	35	40	50
	Average	15	20	30	25	30	40	30	35	45	40	45	55
	Maximum	20	25	35	30	35	45	35	40	50	45	50	60
Sedimentary rock (or coal)	Minimum	30	35	45	40	45	55	45	50	60	55	60	70
	Average	55	60	70	65	70	80	70	75	85	80	85	95
	Maximum	70	75	85	80	85	95	85	95	100	95	100	110
Timbered (5-foot centers)	Minimum	80	85	95	90	95	105	95	100	110	105	110	120
	Average	95	100	110	105	110	120	110	115	125	120	125	135
	Maximum	105	110	120	115	120	130	120	125	135	130	135	145
Igneous rock	Minimum	90	95	105	100	105	115	105	110	120	115	120	130
	Average	145	150	160	155	160	165	160	165	175	170	175	195
	Maximum	195	200	210	205	210	220	210	215	225	220	225	235

Values of $K \times 10^{10}$, lb.-min²/ft⁴

Table 2.2.3(b): U.S.B.M. schedule of friction factors for mine airways in SI units

Type of airway	Irregularities of surfaces, areas, and alignment	Values of K kg/m³											
		Straight			Sinuous or curved								
					Slightly			Moderately			High degree		
		Clean (basic values)	Slightly ob-structured	Moder-ately ob-structured	Clean	Slightly ob-structured	Moder-ately ob-structured	Clean	Slightly ob-structured	Moder-ately ob-structured	Clean	Slightly ob-structured	Moder-ately ob-structured
Smooth lined	Minimum	0.0019	0.0028	0.0046	0.0037	0.0046	0.0065	0.0046	0.0056	0.0074	0.0065	0.0074	0.0093
	Average	0.0028	0.0037	0.0056	0.0046	0.0056	0.0074	0.0056	0.0065	0.0083	0.0074	0.0083	0.0102
	Maximum	0.0037	0.0046	0.0065	0.0056	0.0065	0.0083	0.0065	0.0074	0.0093	0.0083	0.0093	0.0111
Sedimentary rock (or coal)	Minimum	0.0056	0.0065	0.0083	0.0074	0.0083	0.0102	0.0083	0.0093	0.0111	0.0102	0.0111	0.0130
	Average	0.0102	0.0111	0.0130	0.0121	0.0130	0.0148	0.0130	0.0139	0.0158	0.0148	0.0158	0.0176
	Maximum	0.0130	0.0139	0.0158	0.0148	0.0158	0.0176	0.0158	0.0176	0.0186	0.0176	0.0186	0.0204
Timbered (5-foot centers)	Minimum	0.0148	0.0158	0.0176	0.0167	0.0176	0.0195	0.0176	0.0186	0.0204	0.0195	0.0204	0.0223
	Average	0.0176	0.0186	0.0204	0.0195	0.0204	0.0223	0.0204	0.0213	0.0232	0.0223	0.0232	0.0250
	Maximum	0.0195	0.0204	0.0223	0.0213	0.0223	0.0241	0.0223	0.0232	0.0250	0.0241	0.0250	0.0269
Igneous rock	Minimum	0.0167	0.0176	0.0195	0.0186	0.0195	0.0213	0.0195	0.0204	0.0223	0.0213	0.0223	0.0241
	Average	0.0269	0.0278	0.0297	0.0288	0.0297	0.0306	0.0297	0.0306	0.0325	0.0315	0.0325	0.0362
	Maximum	0.0362	0.0371	0.0390	0.0380	0.0390	0.0408	0.0390	0.0399	0.0417	0.0408	0.0417	0.0436

Kharker, Ramani and Stefanco[10] etal surveyed five coal mines in Pennsylvania, West Virginia and Virginia and 108 roadway segments, to find friction factors for coal mines. Their results are shown in Table 2.2.3(c) and a SI version of their results are given in Table 2.2.3(d):

Table 2.2.3(c): Friction factors for US coal mines

	Values of $K \times 10^{10}$, lb-min^2/ft^4					
	Straight			Curved		
Type of airways	Clean	Slightly obstructed	Moderately obstructed	Clean	Slightly obstructed	Moderately obstructed
Smooth lined	25 10, 15, 20	28 15, 20, 25	34 25, 30, 35	31 25, 30, 25	30 30, 35, 40	43 40, 45, 50
Unlined or roof bolted	43 30, 55, 70	49 35, 60, 75	61 45, 70, 85	62 45, 70, 85	68 50, 75, 95	74 60, 85, 110
Timbered	67 80, 95, 105	75 85, 110, 110	82 95, 110, 120	85 95, 110, 120	87 110, 115, 125	90 110, 125, 135

Notes: All values of K for air weighting 0,0750 lb/ft^3. Values in the table are expressed in whole numbers must be multiplied by 10-^{10} to obtain the proper K value.

Table 2.2.3(d): Friction factors for US coal mine airways in SI units

	Values of K kg/m^3					
	Straight			Curved		
Type of airways	Clean	Slightly obstructed	Moderately obstructed	Clean	Slightly obstructed	Moderately obstructed
Smooth lined	0,0046	0,0052	0,0063	0,0058	0,0056	0,0080
Unlined or roof bolted	0,0080	0,0091	0,0113	0,0015	0,0126	0,0137
Timbered	0,0124	0,0139	0,0152	0,0158	0,0161	0,0167

The underlined values in Table 2.2.3(c) are the minimum, average and maximum values of friction factors that McElroy obtained for similar conditions during his investigations as shown in Table 2.2.3(a).

In 1976 Rahim et al[11] carried out field investigations to determine the 'K' value for different roadway conditions in Indian mines. Their results were based on an investigation of six different types of airways. The cross sectional area of the airways varied between 4,13 and 15,64 m^2. The work was done at a mechanised coal mine in the Jharia coalfield; all the measurements were carried out during normal working hours. The actual values for 'K' are presented in Table 2.2.3(e):

Table 2.2.3(e): Coefficient of friction for different airways in Indian Mines

Class of Roadway	'K' Value	
	Range	Average
Unlined/unsupported airways in coal	0,00077 - 0,00126	0,00105
Airways Supported with Roof Bolts	0,00083 - 0,00201	0,00153
Airways Supported with Steel Arches	0,00112 - 0,00159	0,00139
Airways Supported with Steel beams on Concrete Walls	0,00125 - 0,00140	0,00132
Airways Supported with Props and Bars	0,00224 - 0,00319	0,02259

The average value of 'K' for roof bolted airways is 46 % higher than for unlined airways. Similarly, the use of steel beams supported on concrete walls and steel arches showed an increase of 26 % and 36 % respectively over unlined airways. The latter two classes of airways had scattered stocks of material at places.

Rahim et al[11], furthermore, published a list of previously published values of 'K' for different types of airways as determined by various investigators. It is given in Tables 2.2.3(f), 2.2.3(g) and 2.2.3(h). Their results are:

Table 2.2.3(f): Coefficient of friction for unlined airways in Indian Mines

Condition of Airway		Value of 'K' $(kg\ sec^2/m^4)$	Source
Unlined levels:	Uniform section no obstruction	0.00037	Devillez[A]
	Straight (1.8x2.4m) approx.	0.00069	Greenwald[A]
	Even section driven in coal	0.00053	Elween[A]
	Irregular section driven in coal	0.00069	Elween[A]
	Regular section, very jagged sides	0.00089	Elween[A]
	Very irregular driven in coal	0.00106	Elween[A]
Unlined Tunnel:	Igneous rock	0.00302	Frost[B]
	Sedimentary rock or coal	0.00113	Frost[B]
	Unlined airway	0.00076	Frost[B]
	Altofts airway (unlined)	0.00062	Cooke and Statham[C]
	Unlined stone drift in coal measure strata	max.: 0.00106 min.: 0.00091	Vogel[D]
Unlined Galleries:	Straight normal area	0.00093	Murgue[E]
	Straight normal area	0.00087	Murgue[E]
	Straight large area	0.00105	Murgue[E]
	Straight small area	0.00123	Murgue[E]
Sedimentary Rock or Coal:	Straight and clean	min.: 0.00057 Avg.: 0.00103 max.: 0.00132	McElroy & Richardson[F]
Sedimentary Rock or Coal:	(Sinuous or curved airways) Straight and clean	min : 0.00076 Avg : 0.00123 max : 0.00151	McElroy & Richardson[F]
Untimbered roadways with natural sides		0.00132	Cooke and Statham[G]
Unlined straight airway with fairly uniform sides		0.00123	NCB[H]
Unlined airways with rough or irregular conditions		0.00161	NCB[H]
Coal Mines:	Airways driven in rock, across strike	0.0010	Komarov and Skochinsky[I]
	Airways driven in rock, along strike	0.0008	Komarov and Skochinsky[I]
	Levels driven in the coal of regular shape without ripping the roof or the floor	0.4005-0.0006	Komarov and Skochinsky[I]
	Level driven in coal of regular shape with ripping	0.0007-0.0008	Komarov and Skochinsky[I]
	Airways in coal	0.0008	Komarov and Skochinsky[I]
Metal Mines:	Airways (unsupported) driven along the strike: for angle of dip 60-75° for angle of dip 75-90°	0.0012 0.0010	Romensky[I]
	Airways (unsupported) driven across the strike: when air moving up the dip (angle of dip 60-75°) when air moving up the dip (angle of dip 75-90°) when air moving down the dip (angle of dip 60-75°) when air moving down the dip (angle of dip 75-90°)	0.0017 0.0013 0.0022 0.0020	Romensky[I]
Unsupported airways in Limestone beds		min.: 0.00069 max.: 0.00133 avg.: 0.00098	Vujec[J]

25

Table 2.2.3(g): Coefficient of friction values for steel arched roadways in Indian Mines

Condition of Steel Arch Lining	Value of 'K' $(kg\ sec^2/m^4)$	Source
Arch girded roadway	0.00157	Williamson[K]
Steel arch roadway	0.00074	Schmidt[K]
Steel arch girdered airway lined with brick work to spring	0.00042	Clive[L]
Steel arch girdered lined with timber over arches	0.00112	Clive[L]
Steel arch girdered return gate near face	0.00123	Clive[L]
Bricked between arches all round	0.00057	Hinsley[I]
Bricked between arches to spring	0.00076	Hinsley[I]
Lagged with timber at the back fairly smooth	0.00094	Hinsley[I]
Average conditions (main airways)	0.00103	Hinsley[I]
Rather rough conditions (gate roads)	0.00123	Hinsley[I]
Arches poorly aligned, sagged	0.00151	Hinsley[I]
Smooth concrete all round	0.00038	NCB[H]
Concrete slabs or timber lagging between flanges all round	0.00075	NCB[H]
Rough conditions with irregular roofs, sides, and floors	0.00161	NCB[H]
Gangway supported with Alphine E-21 or molls supports (steel arch) at every 0.6-0.7 m.	min.: 0.00156 max.: 0.00200 avg.: 0.00186	Vujec[J]
Perfectly straight arched roadway	0.00062	Houberchts[K]
Main return arched roadway, with subsidence high air speed	0.00189	Houberchts[K]
Main intake, arched roadway	0.00123	Houberchts[K]
Nearly straight arched roadways, irregular section, major arched obstructions	0.00153	Houberchts[K]

Table 2.2.3(h): Coefficient of friction values for timbered airways in Indian Mines

Condition of Airway	Value of 'K' $(kg\ sec^2/m^4)$	Source
Straight, normal area	0.00170	Murgue[E]
Straight, normal area	0.00147	Murgue[E]
Slightly-sinuous, small area	0.00241	Murgue[E]
Timbered airway 1.5m center: straight and clean	min.: 0.00151 avg.: 0.00180 max.: 0.00161	McElroy and Richardson[F]
straight slightly obstructed	min.: 0.00161 avg.: 0.00190 max.: 0.00209	McElroy and Richardson[F]
moderately obstructed	min.: 0.00180 avg.: 0.00209 max.: 0.00230	McElroy and Richardson[F]
Regular section in coal, heavily timbered	0.00091	Elween[A]
Irregular section in coal, heavily timbered	0.00106	Elween[A]
Rockingham airway, regular section	0.00214	Hay and Cooke[M]
Altofts airway, timber set 9.6m apart	0.00121	Cooke and Statham[C]
Altofts airway, timber set 4.8m apart	0.00152	Cooke and Statham[C]
Timbered airway (1.5m center)	0.00189	Frost[B]
Airway with slight turns, tight timbering	0.001	Rees[B]
Wood bars or steel girders on timber legs	0.00189	NCB[H]

Wala[5] assessed the friction factor for 10 coal mines in Kentucky. He collected data that was used to:

♦ validate the Colebrook equation

♦ determine values for surface roughness for airways in bord and pillar mines.

♦ determine friction factors for different mining conditions.

The results of his work are presented in Table 2.2.3(i). The table is a reproduction of Wala's table with a column added to give "K" in SI units. A reworked graph in SI units, that gives the relationship found between Atkinson's friction factor and entry height, is shown in Figure 2.2.3(a). The graphs are applicable for new, clean, straight, unobstructed and roofbolted airways. A 35 % difference in K-factor was found between low (under 1,2 m) and high (above 1,8 m) coal seams. A further mentionable influence was the condition of the floor. When the floor was covered with broken roof rocks or was a rough hard muddy floor, the k-factor was up to 50 % higher.

Table 2.2.3(i): Data from the Wala investigation in Kentucky Mines

| Mining Method	Height of Entry (ft)	A (ft^2)	P (ft)	D=4A/P (ft)	R$_N$ *10^5	k	K *10^{-10} (lb*min^2/ft	K (kg/m^3)	e (inch)	e/D
Continuous	8,2	154	55	11,4	4,76	0,0040	26	0.00482	0,78	0,0058
Miners "clean"	6,5	133	53	10,0	6,82	0,0031	20	0.00371	0,30	0,0024
	4,1	76	48	6,3	2,35	0,0059	34	0.00631	1,4	0,0187
	3,3	53	41	5,2	2,76	0,0053	35	0.00649	0,87	0,014
	3,8	76	47	6,5	1,65	0,0052	34	0.00631	1,1	0,0137
Conventional	3,9	77	47	6,5	4,57	0,0048	31	0.00575	0,9	0,0116
Method	4,8	98	48	8,2	2,22	0,0084	54	0.01002	4,3	0,044
	7,1	135	52	10,3	5,36	0,0061	39	0.00723	2,3	0,0187
	5,6	79	46	6,8	1,54	0,0071	45	0.00835	2,5	0,0299
Continuous	9,0	175	58	12,0	4,16	0,0100	66	0.01224	9,8	0,068
Miners "rough"	5,6	107	52	8,3	0,72	0,0084	49	0.00909	4,3	0,043
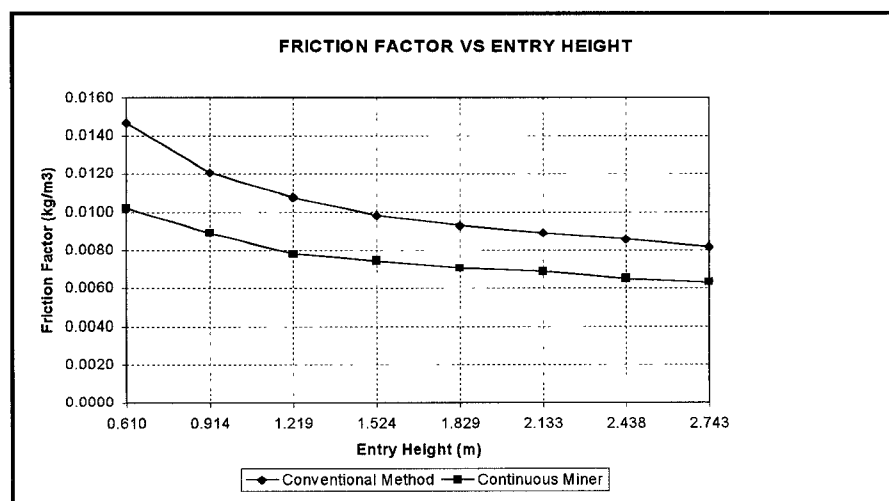
Figure 2.2.3(a): **Friction factor as a function of entry height for Kentucky bord and pillar mines**

McPherson[12] published a short list of friction factors in 1975, which is presented in Table 2.2.3(j). He also provided a nomogram, Figure 2.2.3(b), that can be used to determine the resistance of a roadway. The nomogram is based on a circular cross section. By multiplying with a relative shape factor, Table 2.2.3(k), the resistance of other shaped airways can be determined.

Table2.2.3(j): McPherson's list of K-values

Type of airway	Characteristics of airway	K (kg/m^3)
Shafts	Smooth, concrete lined, clean	0,0030
	Brick lined, clean	0,0037
	Smooth, concrete lined, rope guides and pipe ranges on bunions	0,0065
	Brick lined, rope guides and pipe ranges on buttons	0,0074
	Tubbing lined, no guides or cages	0,0139
	Timber lined, no middle buttons	0,0167
	Brick lined, 2 lines of side buttons, without tie girders	0,0176
	Brick lined, 2 lines of side buttons, 1 tie girders to each bunton	0,0223
	Timber lined with middle buttons	0,0223
Steel Arched Roadways	Smooth concrete all round	0,0037
	Concrete slabs or timber lagging between flanges all round	0,0074
	Concrete slabs or timber lagging between flanges to spring	0,0093
	Lagged behind arches, good condition	0,0121
	Rough conditions with irregular roof, sides and floor	0,0158
Rectangular roadways	Smooth concrete lined	0,0037
	Girders on brick or concrete walls	0,0093
	Unlined airways with uniform sides	0,0121
	Unlined airways, irregular conditions	0,0158
	Girders or bars on timber props	0,0186

Table 2.2.3(k): Relative shape factor

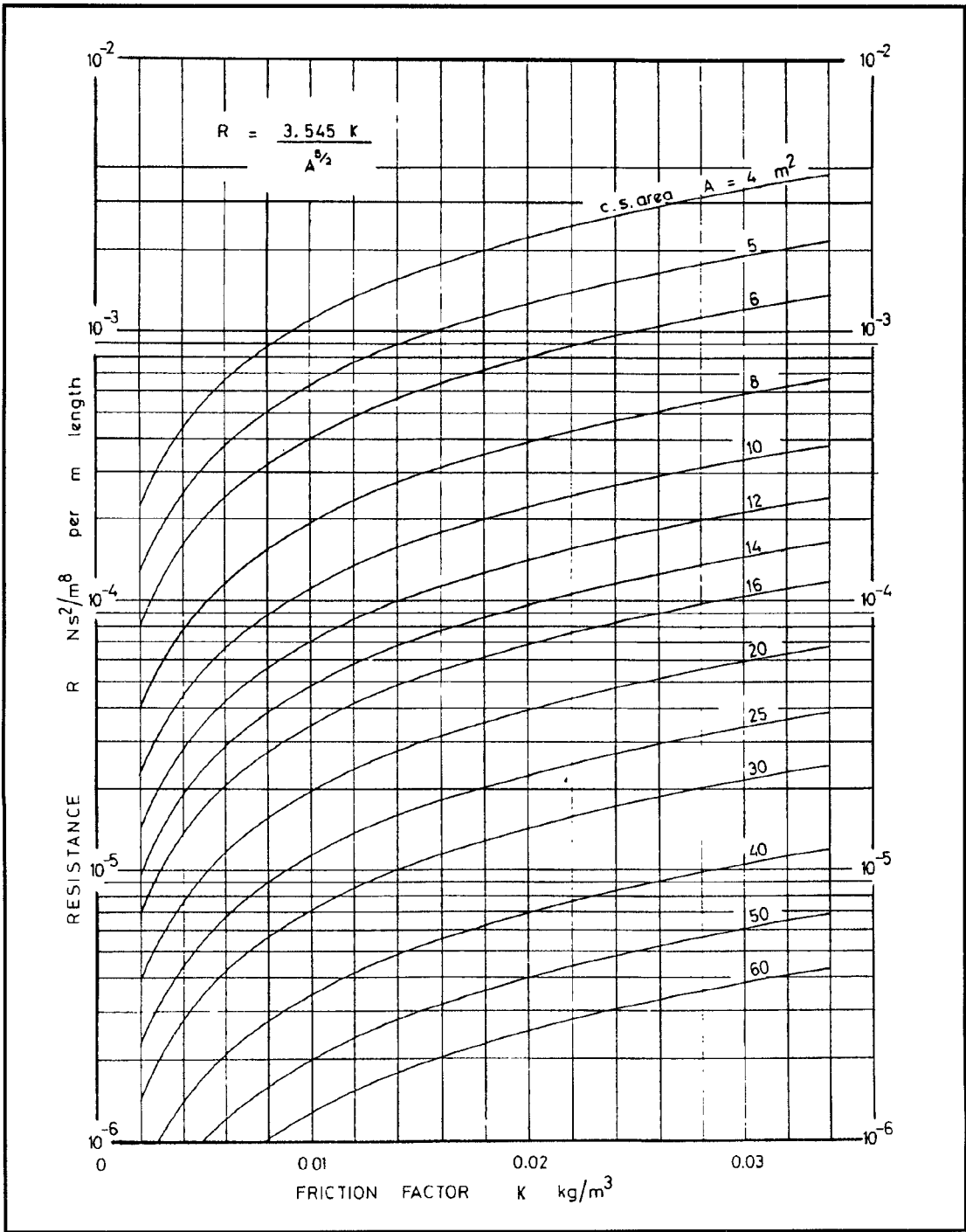| Shape of Roadway or Shaft	Factor
Circular	1,00
Arched, straight legs	1,08
Arched, splayed legs	1,09
Square	1,13
Rectangular width : height = 1,5 : 1	1,15
2 : 1	1,20
3 : 1	1,30
4: 1	1,41

Figure 2.2.3(b) Resistance nomogram for circular airways and standard air density

29

The Reynolds numbers for the results obtained by Deglon and Hemp[7] were between 340 00 and
1 200 000, and the air densities between 1,000 kg/m^3 and 1,032 kg/m^3. Their results are represented in
Table 2.2.3(l), and the average value for friction factor was 0,0087 (Ns^2/m^4). They felt that the high
value for no 5 was the result of shock losses occurring at a number of right angled bends and
restrictions in the section. The value for no. 6 could not be explained as the result in no. 7 was taken at
the same location six months later.

Table 2.2.3(l): Results of Deglon and Hemp investigations

Survey No.	Length of section (m)	Average Width (m)	Average Height (m)	Pillar centres (m)	No. of Roadways	Pressure Loss (Pa)	Quantity (m^3/s)	K factor (Ns^2/m^m)
1	1000	5,98	1,95	30,5	2	14,1	27,2	0,0091
2	842	6,13	2,02	15,4	5	34,4	124,4	0,0091
3	90	5,05	3,20	13,0	1	16,6	84,6	0,0078
4	90	5,05	3,20	13,0	2	4,6	85,1	0,0086
5	380	6,07	2,45	36,0	1	70,2	51,4	0,0157
6	392	6,15	2,55	36,0	1	25,0	34,9	0,0134
7	392	6,15	2,55	36,0	1	36,0	51,0	0,0091

From the data Martinson[8] obtained, they determined the value of the Atkinson and Darcy friction
factors for different sections in the Trona mine. Their results are presented in table form in Table
2.2.3(m).

Table 2.2.3(m): Values obtained for a Trona mine

Length of airway segment (m)	Reynolds Number	Darcy friction factor	Atkinson's friction factor (Ns^2/m^4)
457,2	208 000	0,0525	0,00788
457,2	231 000	0,0722	0,0109
457,2	253 000	0,0657	0,00987

2.3 Shock losses

Shock losses are the result of changes in direction and/or changes in cross-sectional areas of mine
airways. The major cause of shock losses in an underground mine can be attributed to one of the
following:

- ◆ Overcasts and Shafts
- ◆ Splits and Junctions
- ◆ Bends and Turns

2.3.1 Theory

Shock losses are independent of the roughness of walls and can thus not be computed directly as is the case with friction losses. The three methods for determining shock losses are:

1. As a function of velocity pressure.

   $$P_x = XP_v$$

   with P_x the pressure loss due to a shock and X an empirical shock loss factor that is determined experimentally.

2. Increasing the value of the friction factor for the section of the airway where the shock losses occur.

3. Expressing the shock loss as an additional length that is added to the length of the airway.

Overcasts (Aircrossing)

An overcast is an air bridge which allows two air currents to cross each other without mixing with one another. It is one of the major sources of shock losses underground. However money can be saved if the planning and construction of overcasts are done in such a way that they minimise the shock loss. The errors that are commonly made in the construction of overcasts are that they cause rough and abrupt interruption of the ventilating current and insufficient area. Two types of shock losses are caused by this unfavourate construction of overcasts. The first is due to sudden velocity changes. When the air reaches the overcast, the size is normally reduced, and the air has to squeeze through a much smaller area. This will reduce the airflow, which will result in pressure loss due to the sudden contraction and expansion. The amount of loss is dictated by the ratio of the reduced area to the area preceding the bottleneck, and can be derived from Bernoulli's theorem. The second type is due to turns. When air moves around a bend it experiences a centrifugal force. The result of this centrifugal force is a transverse pressure gradient, which is not confined to the actual bend, but extends some two to three diameters upstream and downstream from the bend. The air tends to crowd to the far side of the bend and occupies less than the full area available. When the air once more expands to the full area, following the bend, a shock loss occurs.

Shafts

McPherson[13] reported on the findings of an investigation by the United States into the design of mine shafts. The resistance to airflow, R, offered by a mine shaft is influenced by four factors. The factors and their influences are briefly discussed in the following:

a) Shaft Walls. **By using equation (1) and making the necessary substitutions the shaft wall resistance can be determined by the following:**

$$r_W = \frac{f}{2} \frac{LO}{A^3} \qquad (10)$$

b) **Shaft Fittings.** The fittings in a shaft can be grouped into two groups. The first group concerns longitudinal fittings; this group adds to the resistance to flow in that it reduces the area that is available for flow. The contribution to frictional drag is small compared to the large surface area of the shaft walls. The second group concerns items that are perpendicular to the direction of airflow. Members of this group include buntons and cross-members. The resistance for a single bunton is given by:

$$r_{1b} = C_D \frac{A_b}{2A^3} \qquad (11)$$

with
$$C_D = \text{coefficient of drag}$$
$$A_b = \text{projected area facing into the airstream}$$

The resistance of a single bunton should be multiplied by the total number of buntons in the shaft. Equation (11) does not take into account the influence of turbulent eddies that a bunton will have on the following bunton if they are not spaced far enough for the eddies to have died out.

c) **Conveyances.** The resistance of a cage is considered in two parts: the first is due to the obstruction of airflow by a stationary conveyance and the second concerns the effects caused by the motion of the conveyance. The resistance of a stationary cage, expressed in terms of a shock factor X, is given by:

$$r_c = \frac{X}{2A^2} \qquad (12)$$

Methods of determining the shock loss X are presented by McPherson[Error! Bookmark not defined.] in his paper. When the conveyance is moving at a velocity u_c, against an airflow velocity of u_a, the effective resistance of the cage will oscillate between a maximum value, when the cage is moving against the airflow, and a minimum when it is moving with the airflow. The effective resistance is then given by:

$$r_{ceff} = r_c \left[1 \pm \frac{u_c^2}{u_a^2} \right] \qquad (13)$$

Inserts, Loading and Unloading Points. The shock losses at these locations in the shaft can be converted into resistance through:

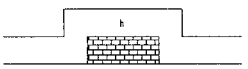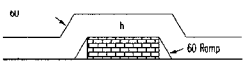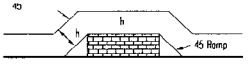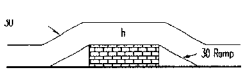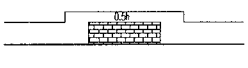$$r_{sh} = \frac{X}{2A^2} \qquad (14)$$

32
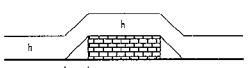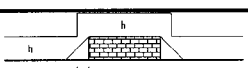
The overall shaft resistance for a shaft with a conveyance is given by a combination of the above values for resistance:

$$r_{tot} = r_w + r_b + r_c\left[1 \pm \frac{u_c^2}{u_a^2}\right] + r_{sh} \qquad (m^{-4}) \qquad (15)$$

2.3.2 Measurements and results

In 1987 Tien[14] used a physical model to determine the shock losses for different overcast constructions. The Reynolds number for his model was 1 641 062, which is in the turbulent range. The results of Tien's[14] work are summarised in Table 2.3.2(a).

Table 2.3.2(a): Shock losses around overcasts

	Total Press. H_t, (Pa)	Press. Drop ΔH, (Pa)	Velocity (m/s)	Quality (m^3s)	Flow Index (m^3s/Pa)	Equivalent Length (m)	Set-up
90° Roof							
w/ ramp	131,27	113,83	5,20	0,61	5,37	179,1	
w/o ramp	131,34	79,96	3,77	0,44	5,55	7,2	
60° Roof							
w/ Ramp	57,04	16,94	4,38	0,52	30,40	0,6	
w/o Ramp	58,54	18,93	3,95	0,47	24,58	2,2	
45° Roof							
w/Ramp	53,06	17,44	4,53	0,53	30,56	0,4	
w/o Ramp	58,04	19,68	4,09	0,48	24,46	1,8	
w/ Stair	57,79	18,43	4,38	0,52	27,96	0,8	
30° Roof							
w/ Ramp	50,81	9,47	4,67	0,55	58,04	0	
w/o Ramp	53,80	17,19	5,29	0,62	36,22	0	
w/ Stair	53,80	17,19	4,63	0,54	31,66	0,2	
Half Height							
w/o Ramp	123,05	88,68	8,81	0,52	5,85	10,7	
w/ Ramp	107,36	68,75	4,07	0,48	6,97	11,4	
w/o Ramp	106,11	68,25	4,41	0,52	7,61	23,7	
w/ Ramp	380,86	394,56	1,57	0,19	0,47	494,8	
w/o Ramp	219,45	197,28	1,84	0,22	1,10	129,0	

The flow index is the ratio between the air quantity and pressure drop across the overcast. In the table the "flow index" is used as a method of comparison. By comparing the flow index, the influence of adding a ramp and the best angle for the ramp can be identified. A higher flow index is an indication that the air quantity is higher. The second last column in the table gives equivalent lengths that can be added to the length of an airway to take the effect of the aircrossing into consideration.

Martinson[8] used pressure and flow measurements to calculate the shaft friction factors and collar shock loss factors; the results are presented in Table 2.3.2(b).

Table 2.3.2(b): Shock loss and friction factors for a shaft in a Trona mine

Wall Leakage Percent	Collar		Shaft 50 - 300 ft	
	Flowrate ft^3/min	CSLF* k	Flowrate ft^3/min	SFF** (K) (Ns^2/m^4)
0,0	369 000	1,76	368 100	0,00764
2,5	378 500	1,62	377 600	0,00727
5,0	388 400	1,48	387 500	0,00690
7,5	398 900	1,36	398 000	0,00653
10,0	410 000	1,23	409 000	0,00620

* COLLAR SHOCK LOSS FACTORS   ** SHAFT FRICTION FACTORS

The density at the collar at 50 ft was 0,0587 lb/ft^3 while at 300 ft below the collar the density was 0,0589 lb/ft^3. The leakage factors were included for illustrative purpose. The shaft was a 6,1 m diameter, concrete lined vertical shaft divided into equal downcast and upcast compartments by a 203 mm wall installed on a shaft diameter. Exhaust fans at the top of the upcast compartment generate a pressure difference of 2,30 kPa. In the downcast compartment is a two deck cage balanced by a counterweight.

2.4 Remarks

This study was not intended to offer anything new or original, but merely to collate as much as possible of the information that is available on the subject and to provide the industry with values that have been obtained by others investigating the same subject.

Calculation of roadway resistance on the basis of published values of 'K' yields results with significant deviations. Moreover the conditions to which the published values relate are not always elaborated on. Thus there is a need to collect more specific and detailed information on the values of 'K' for different roadway conditions.

Furthermore since the K - factor is site dependent, comprehensive field investigations are required to determine these values in - situ for existing mining conditions in South African collieries. From these results tables and graphs should be drawn up that can be used as a reference by the industry.

From the investigation on shock losses it was found that for an overcast with ramps, the more gradual the ramp, the smaller the change in air velocity, resulting in smaller shock losses.

3   Underground Observations

3.1   Introduction

Studying the information that was gathered from the literature study, a vast amount of information is avaliable to the ventilation practitioner that can be used when planning the ventilation of any coal mine. If this information is evaluated more critical, it might prove that some of it could be applicable to SA conditions and could therefore be of great importance to any environmental control department. Whether to use the information supplied in the literature study will have to be decided by the individual mines and groups and should be evaluated under specified conditions.

To be able to provide values that could be of easy and practical use to the ventilation departments in SA collieries, it is necessary to supply information on typical values that were determined under SA mining conditions and in a format that could be used with ease and confidence. The next section describes the work that was carried out in typical underground bord and pillar conditions and also results that were obtained from using the aid of CFD simulations.

3.2   Test procedures

All the underground measurements were carried out using the trailing hose method where a certain length of tubing is used to measure the direct pressure difference between two points as described by Le Roux[15]. The 6 mm Ø plastic tubing was laid in position at least 24 hours before the actual test was performed to enable the air inside the tube to adjust to the atmosphere outside the tube. The pressure measurements were then taken by connecting the one end of the tube to an electronic manometer that gave a direct reading of the air pressure present inside the tube as a result of the prevailing airflow.

When measuring the pressure loss in an intake or return airway, the length of the tubing that should be used is determined by the amount of airflow in the particular roadway or section being tested. It is often difficult to achieve a decent pressure loss over a given distance if the air velocity is too low. The lower the air velocity, the more difficult it is to achieve a high enough pressure difference between the two points. It was found that air volumes of more than 60 m^3/s are needed per roadway to be able to obtain a reading over a distance of at least 200 m of tube length. If the air volume is lower, the test section and therefore the tube length must increase. During the actual testing, it was necessary to sometimes extend the tube length and repeat the test to obtain more accurate results.

At the position where the pressure difference was measured, the following additional measurements were also made:

- prevailing air quantity flowing through the test section

- airway dimensions where the actual measurements were made

- air temperature and atmospheric pressure for calculating the actual air density

- exact length of the test section

During all these measurements, control barometer measurements were recorded and the elevations of the measuring points were gathered from the survey departments.

With all this information in hand, it was possible to determine the actual friction factor for the particular test section or roadway using the Atkinson's formula (combination of equation 1 and 6).

The actual air density that was used, was determined by using the equation:

$$p = wRt \qquad (16)$$

where   p = atmospheric pressure (kPa)

w = air density (kg/m^3)

R = 0,287(gas constant)

t = temperature (kelvin)

During the measurements of intake and return airways, the presence of walls and stoppings made the accuracy of the measurements more difficult due to air leakage and obstructions. To be able to provide pratical results that would be representative to the underground conditions, it was necessary to prepare the test sections and remove any unwanted obstructions and interference from the roadways.

Although leakage characteristics through the walls and stoppings is also important for planning ventilation requirements, it was important to minimise the amount of air leakage for measuring the friction loss for a specific airway section. To achieve this, the walls were covered with sealants and also ventilation brattices before the tests were carried out. The determination and use of air leakage characteristics through stoppings and aircrossings and the development of a computer program that can determine the planning values needed for specific conditions, has been fully investigated and documented (Hemp & Deglon)[7].

Details on which underground measurements should be taken, the type and amount of measurements that should be taken as well as the way this information is used for calculating pressure losses and friction factors are described in detail by Le Roux[15] and in the Environmental Control Text Book[16]. The detail will therefore not be discussed again in this document.

3.3 Test results

To date, the industry has been using basic friction values for conducting network simulations for the purpose of long term and medium term planning as well as for evaluating the current ventilation network of the mine or colliery. These values were normally taken either from charts used by the USBM (see Table 3.3) or from values that were provided by some research organisations and mining houses as being accurate and reliable. Values such as $0,0015 \text{ Ns}^2/\text{m}^4$ are used for any intake airway and a value of $0,018 \text{ Ns}^2/\text{m}^4$ is used for any return airway. A more accurately determined value of $0,0087 \text{ Ns}^2/\text{m}^4$ (Hemp & Deglon)[7] has been used with more confidence and with a limited degree of success.

All results that are tabulated in this report have been converted to standard air density of $1,2 \text{ kg/m}^3$.

Table 3.3   Set of friction values as supplied by the USBM

PRESSURE DROP PER 100 METRES OF MINE AIRWAY	
VALUES OF "K" FOR CIRCULAR AIRWAYS	
SHAFTS	**Ns^2/m^4**
Smooth concrete-lined, unobstructed	0,0030
Brick-lined, unobstructed	0,0037
Smooth concrete-lined, with rope guides and pipe ranges on buntons	0,0065
Brick-lined, with rope guides and pipe ranges on buntons	0,0074
Tubbing-lined, with no guides or cages	0,0139
Timber-lined, no middle buntons	0,0167
Brick-lined, two lines of side buntons, without tie girders	0,0176
Brick-lined, two lines of side buntons, one tie girder to each bunton	0,0223
Timber-lined, with middle buntons	0,0223
STEEL ARCHED ROADWAYS	**Ns^2/m^4**
Smooth concrete all round	0,0037
Concrete slabs or timber lagging between flanges all round	0,0074
Concrete slabs or timber lagging between flanges to spring	0,0093
Lagged behind arches, good condition	0,0121
Rough conditions with irregular roof, sides and floor	0,0158
RECTANGULAR ROADWAYS	**Ns^2/m^4**
Smooth concrete-lined	0,0037
Girders on brick or concrete walls	0,0093
Unlined airways with uniform sides	0,0121
Unlined airways irregular conditions	0,0158
Girders or bars on timber props	0,0186

To be able to perform more accurate and effective planning and evaluation exercises, however, the ventilation practitioner needs values that describe in more detail the specific conditions in the mine environment that could influence the overall airflow behaviour through the mine. In the literature study, it was shown that some of the overseas countries have done fairly comprehensive studies into the effect of different aircrossing designs and the effect of corners, doors, intersections, etc. As said before, it could be possible to relate some of this information to SA conditions and perhaps could be incorporated into the basic set of values used by the ventilation practitioner.

Nevertheless, it is still necessary to provide values to the industry that could describe basic underground bord and pillar conditions that could be used in network simulation programs, which would ensure a more reliable end result.

It was for this reason that a number of underground conditions and scenarios were identified that were to be used to determine generic values that could be used in general by all coal mines. After a discussion with some representatives from the various mining groups, it was decided to concentrate on measuring friction values for the following typical scenarios:

- intake and return airways developed by conventional mining methods

- intake and return airways developed by mechanical mining methods

- a value for a typical dyke excavation

- a typical aircrossing installation

- an incline shaft used for travelling or coal conveying or both

- an empty raise-bore shaft

3.3.1   Conventional and mechanical mining methods

To cater in general for all coal mines, tests were carried out in different seam heights in order to obtain values for low seams (<2,0 m), medium seams (2,0 m to 4,0 m) and high seams (>4,0 m). An increase in seam height should theoretically not have an effect on the actual friction value, but the tests have shown that with a difference in seam height, a difference in pillar centres and pillar formation occurs, which influences the pressure loss and therefore the calculated friction loss.

As will be demonstrated in the section that deals with the CFD simulation results, the number of pillars and also the shape of pillars in a length of roadway, influences the overall pressure loss in an airway. As the values given are to be used for planning practical ventilation flow through a mine, practical conditions were measured with regard to the different seam heights and the different K-values calculated are given.

Although the use of conventional mining methods is not as extensive as was the case a number of years ago, it is still necessary to know the difference between areas mined by means of a mechanical miner and by conventional means. Because of the large variations between how the coal seams are mined, the surface formation of the coal is also different and therefore the surface roughness will also be different.

Where possible, valuable information was gathered from the mines on individual tests performed and the results were evaluated for accuracy and reliability. Some of these results were used to complete the determination of friction losses for airways developed by means of conventional methods. The measurements in the bord and pillar workings were carried out in areas that differed from 1 road development to as many as seven roads with the roadway widths varying between 4,0 m and 7,0 m.

Listed below in Table 3.3.1(a) are the average roadway conditions that were used to calculate friction losses for conventional bord and pillar mining as given in Table 3.3.1(b). The actual details of the underground tests and individual measurements will not be described and listed in this report. The final value as calculated for intake and return airways for conventional and mechanical mining derived from various underground surveys will be presented.

The average values were calculated out of a total of 60 sets of underground measurements that were taken in various coal mines. Air quantities that were used varied between 20,0 m^3/s to as high as 312 m^3/s. For the seam heights below 2,0 metres, the range of values were between 1,2 m and 1,97 m. The medium range of seam heights between 2,0 m and 4,0 m represents the majority of seam heights in the industry. During the underground observations, the seam heights that were used for the measurements and calculations varied between 2,02 m and 3,65 m. For the high seams, scenarios differed from 3,95 m to 4,43 m.

The length of the test sections were determined by the physical conditions and mining parameters and varied between 249 m and 1000 m.

Figure 3.3.1(a) shows a typical layout of a three road bord and pillar section with the airflow patterns and the typical positions where the measurements were made.

Table 3.3.1(a):   *Average measurement data for conventional mining*

| CONVENTIONAL BORD AND PILLAR MINING				
LOW SEAM MINING (<2,0 m)				
Intake Airways				
Roadway Width (m)	Roadway Height (m)	Airway Length (m)	Pressure Drop (Pa)	Air Quantity (m³/s)
6,5	1,97	500	34,3	67,39
Return Airways				
5,95	1,95	842	33,5	19,6
MEDIUM SEAM MINING (2,0 m to 4,0 m)				
Intake Airways				
6,0	3,4	800	81,4	63,9
Return Airways				
7,2	3,6	300	20,0	210,7
HIGH SEAM MINING (>4,0 m)				
Intake Airways				
7,6	4,5	490	19,89	72,63
Return Airways				
6,9	4,0	1000	25,0	42,1
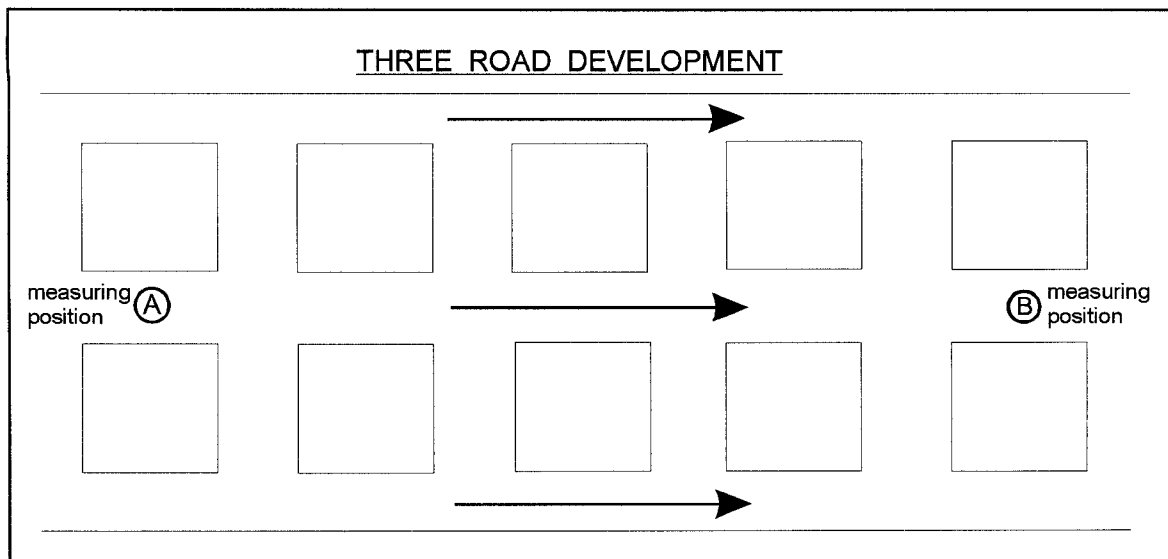
Figure 3.3.1(a) Three road development demonstrating the two measuring positions for determining the pressure difference for k-factor calculations

Table 3.3.1(b) shows the final results of the measurements made during the investigations into the friction values for conventionally developed airways for the low, medium and high seam categories. The values are given for both intake and return airways. These values can be used by all underground coal mines that practise bord and pillar development. It should be emphasised, however, that these values are generic values that should be used for planning purposes only. Mines that have the need to perform site specific calculations with regard to ventilation, should perform their own detailed measurements and observations.

Table 3.3.1(b): Friction values for conventional bord and pillar mining

CONVENTIONAL BORD AND PILLAR MINING	
LOW SEAM MINING (<2,0 m)	Ns^2/m^4
Intake Airways	0,01107
Return Airways	0,01210
MEDIUM SEAM MINING (2,0 m to 4,0 m)	Ns^2/m^4
Intake Airways	0,01334
Return Airways	0,01467
HIGH SEAM MINING (>4,0 m)	Ns^2/m^4
Intake Airways	0,01482
Return Airways	0,01584

The results show that the return values are higher than the intake values in all the cases. To explain this, it is necessary to explain the prevailing conditions in the return roads compared to the conditions in the intake roads. To obtain practical values, areas were identified where shaling, rooffalls, poor roof conditions and in some cases water accumulations were present in the returns. These conditions are normally found in return roads while intake airways are normally kept clean and free from obstructions and thus the difference in friction loss values between intake and return airways.

Listed below in Table 3.3.1(c) are the average roadway conditions that were used to calculate friction losses for mechanical bord and pillar mining as given in Table 3.3.1(d).

Table 3.3.1(c):   **Average measurement data for mechanical mining**

MECHANICAL BORD AND PILLAR MINING				
LOW SEAM MINING (<2,0 m)				
Intake Airways				
Roadway Width (m)	Roadway Height (m)	Airway Length (m)	Pressure Drop (Pa)	Air Quantity (m³/s)
6,36	1,89	500	43,0	33,98
Return Airways				
6,2	1,76	800	33,0	19,5
MEDIUM SEAM MINING (2,0 m to 4,0 m)				
Intake Airways				
6,0	2,5	500	24,0	33,32
Return Airways				
6,55	2,8	400	37	57,1
HIGH SEAM MINING (>4,0 m)				
Intake Airways				
6,6	4,0	249	19,0	86,68
Return Airways				
7,1	4,2	239	30,0	122,9

Table 3.3.1(d) shows the results from the measurements made in airways that have been mined by means of mechanical miners. From the results it is evident that these values are less than the values as quoted for conventional mining. The reason being that the sides are more even and smooth when they are mined with a mechanical miner than when they are mined with conventional mining methods.

Table 3.3.1(d): Friction values for mechanical bord and pillar mining

MECHANICAL BORD AND PILLAR MINING	
LOW SEAM MINING (<2,0 m)	Ns^2/m^4
Intake Airways	0,0095
Return Airways	0,0104
MEDIUM SEAM MINING (2,0 m to 4,0 m)	Ns^2/m^4
Intake Airways	0,0099
Return Airways	0,0109
HIGH SEAM MINING (>4,0 m)	Ns^2/m^4
Intake Airways	0,0106
Return Airways	0,0117

3.3.2   Development through a dyke area

As dykes and faults appear to be a significant factor in deciding the life of a mine and also the type of mining that should be executed and in which direction mining should be pursued, it is only logical that a series of dykes will have a definite influence on the availability of ventilation in critical areas. Most of the dykes that are encountered in underground coal mines have to be holed through by means of drill and blast methods and in most cases extra support has to be installed to control the poor condition of the roof and sides. These conditions normally would prevail for the full length of a pillar if the dyke happens to run through the middle of such a pillar and these poor conditions result in a higher friction value than would be the case for a normal airway pillar. Conditions are similar for all dykes that are encountered and for this reason it was decided to perform tests on only a few situations that could be obtained and prepared on a few mines.

Again using the trailing hose method as described earlier in the paper, a typical friction and resistance value was obtained for a dyke that was mined through by means of drilling and blasting.

Figure 3.3.2 shows a sketch of a typical dyke scenario in a full pillar length with the appreciation that, if sufficient air can be pushed through this area, a proper pressure loss could be achieved for determining the friction and resistance factors for this type of excavation.
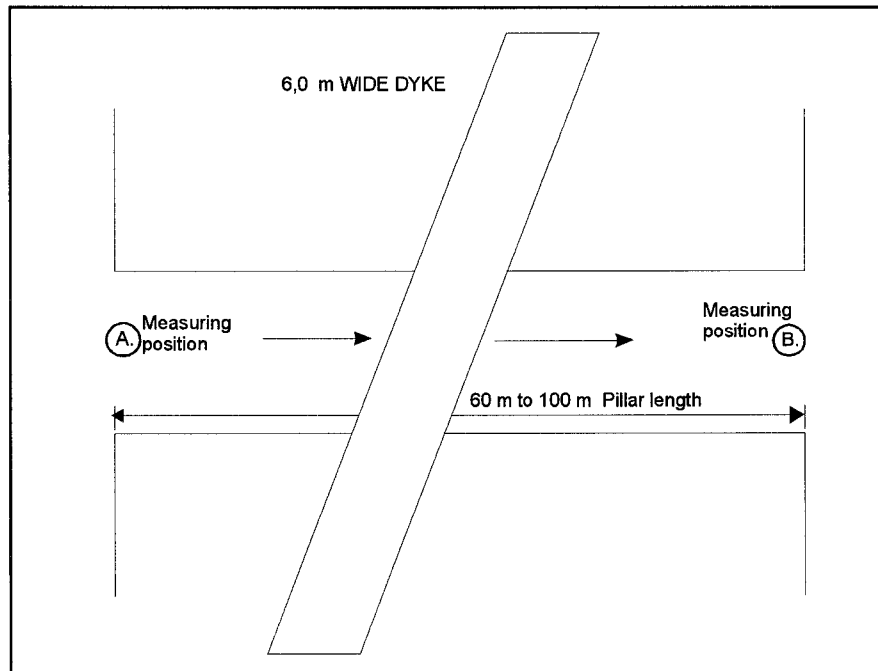

Figure 3.3.2: Sketch showing a typical dyke area as developed through a coal pillar

Derived from the underground observations and measurements, it can be said that for a typical dyke area that is approximately 6 m in width inside a pillar that is in the region of 60 m to 100 m wide, the following friction and resistance values can be used for planning purposes:

♦ RESISTANCE VALUE FOR A TYPICAL DYKE EXCAVATION = 0,02126 Ns^2/m^8

♦ FRICTION FACTOR FOR A TYPICAL DYKE EXCAVATION = 0,0854 Ns^2/m^4

The average underground measurements used for calculating the above values were as follows:

- Roadway width = 5,0 m
- Roadway height = 3,1 m
- Roadway length = 68 m
- Pressure loss = 40,23 Pa
- Air quantity = 43,5 m^3/s

To be able to understand and utilize this value effectively, some calculations will have to be made as per the following example:

* **Example:** The friction factor for a normal bord and pillar roadway in a medium seam developed by means of conventional mining is 0,01334 Ns^2/m^4 (intake air). When a dyke is running through the roadway, the friction value is increased to 0,0854 Ns^2/m^4 for that particular section. Taking into consideration the higher resistance, the pressure loss over this section can be calculated and added to the total pressure loss through the mine. This should then be done for every dyke that is shown and expected on the long term plans due to the geological data. This would mean that the total pressure loss calculated, and therefore the quantity of air needed to ventilate the mine, would be more accurate than in the past.

It must be emphasised again that these values should only be used for planning purposes. Any specific and more accurate values will have to be measured and calculated by the individual mines.

3.3.3   Empty raise-bore shaft

Throughout the years, a great deal of research has been done on the friction values that should be used for vertical shafts (MVS Data Book)[17]. As these values are extremely comprehensive and complete, it was not necessary to perform al of these studies again. Table 3.3.3 below shows all this information that is available to the industry with regard to vertical shafts.

Table 3.3.3: Selection of k-factors for vertical shafts

DESCRIPTION	Ns^2/m^4
Concrete lines-no steelwork	0,004
Smooth lined, unobstructed	0,0037
Brick lined, unobstructed	0,0037
Brick lined, with rope guides and water and air ranges	0,0074
Concrete lined, with streamlined buntons	0,0045-0,025
Tubbing lined shaft with no guides or cages	0,0139
Brick lined shaft with two sets of side buntons	0,0176
Timber lined shaft with a middle line of buntons	0,0223
Concrete lined, with RSJ buntons	0,0075-0,060
Timbered rectangular	0,045-0,09
heavily timbered rectangular	0,08

The need was expressed for a friction factor that could be used for an empty raise bore shaft that could be incorporated in the planning of the mine ventilation. An empty shaft was found and a set of measurements were taken as accurately as possible by means of a trailing hose method. Again all of these were carried out together with all the other measurements that are required for the final calculations. With this particular investigation, use was also made of CFD to verify the experimental work (see chapter on CFD simulations) and also to obtain a clearer picture of what is happening with the air inside the shaft.

Figure 3.3.3 shows a sketch of the shaft with all the relevant information on the airflow and the airway.
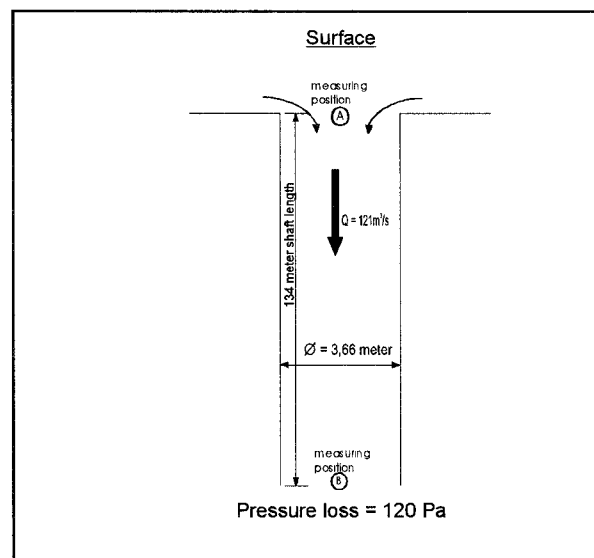

Figure 3.3.3: Sketch showing a typical raise-bore shaft development with all relevant information

The raise bore shaft that was measured was 3,66 m in diameter and a total of 134 m in length. An air quantity of 121 m³/s was flowing down the shaft with a total pressure loss measured as 120 Pa. The friction loss for the shaft was calculated as being:

Total friction loss = **0,00731 Ns^2/m^4**

3.3.4   Typical incline shaft values

In the collieries, incline shafts are used to convey coal, people and air. Incline shafts are therefore an important part of the ventilation distribution network. The amount of resistance to airflow that is caused by the friction characteristics of the shaft has a significant influence on the overall pressure loss of the ventilation system and therefore the main fan system. To date no official information has been available on the effect of the air through an incline shaft on the ventilation distribution. This project concentrated on determining the friction loss inside an incline shaft that is used for coal conveying only, an incline shaft that is used for travelling only and then a combination of both.

The dimensions and parameters inside incline shafts are fairly similar throughout the industry, which means that this generic information that is supplied for incline shafts can be used with confidence for planning purposes throughout the industry. The values are based on the physical underground measurements that were taken in incline shafts.

- INCLINE SHAFT FOR TRAVELLING AND COAL CONVEYING:- Incline shafts can typically be between 3,0 m and 4,0 m in height and between 6,0 m and 7,0 m in width. Fairly high air quantities can flow through these areas and, with the amount of obstructions present inside these airways, significant resistance and friction factors can be determined. The friction loss and resistance factors that were calculated for this scenario are:

Resistance per 100 m = **0,0063 Ns^2/m^8**

Friction loss in shaft = **0,00947 Ns^2/m^4**

The average measurements used for calculating the above values were as follows:

◊   Roadway width = 4,1 m

◊   Roadway height = 3,8 m

◊   Roadway length = 366,6m

◊   Air quantity = 52,0 m^3/s

◊   Pressure loss = 9,0 Pa

- INCLINE SHAFT FOR COAL CONVEYING ONLY:- The mining personnel allowed in an incline shaft that is used for coal conveying only is restricted to maintenance and repair crews. Friction and resistance values may differ due to less obstructions and less rubbing of surfaces. The values that were calculated for this scenario are:

Resistance per 100 m = **0,0033 Ns^2/m^8**

Friction loss in shaft = **0,00741 Ns^2/m^4**

The average measurements used for calculating the above values were as follows:

◊ Roadway width = 4,5 m

◊ Roadway height = 3,7 m

◊ Roadway length = 600,7 m

◊ Air quantity = 73,6 m^3/s

◊ Pressure loss = 12,0 Pa

- INCLINE SHAFT FOR TRAVELLING ONLY:- These airways are mainly open airways that are used for transporting people and air into the mine workings. Rubbing surfaces in this scenario is limited to the roof, sides and floor of the airway with obstructions at a minimum. The results of the measurements in this type of airway are as follows.

Resistance per 100 m = **0,0022 Ns^2/m^8**

Friction loss in shaft = **0,00674 Ns^2/m^4**

The average underground measurements used for calculating the above values were as follows:

◊ Roadway width = 7,1 m

◊ Roadway height = 3,8 m

◊ Roadway length = 536,4 m

◊ Air quantity = 126 m^3/s

◊ Pressure loss = 10 Pa

3.3.5   Typical aircrossing values

The use of an aircrossing in the coal mine ventilation set-up is essential. Air is carried over from one district or airway to another and can only be done by means of an aircrossing. An aircrossing is so-called when the intake and return air cross at a certain position without mixing. The design of such an aircrossing has a significant influence on the restriction and pressure loss of an airstream. Normally the ventilation pressure is destroyed due to shock loss as a result of the physical construction of the aircrossing.

To determine a friction loss or resistance for every type of aircrossing that is available in collieries would comprise a separate project altogether. The decision was therefore made to concentrate on the type of aircrossing design that is most commonly used in the industry, to be able to provide a general value that can be used by the industry for planning purposes.

A series of tests were performed on the intake/fresh air that flows underneath the aircrossing and the same exercise was repeated for the return air that crosses over the aircrossing. The results were obtained over different sets of aircrossings ranging from two to five sets in a single roadway. For this particular scenario it was decided that it would be of more significance to determine a resistance value per aircrossing rather than determining the friction value of an aircrossing. This concept will be explained in more detail. Figure 3.2.5 shows a typical layout design of an aircrossing to explain the crossing of intake and return air.
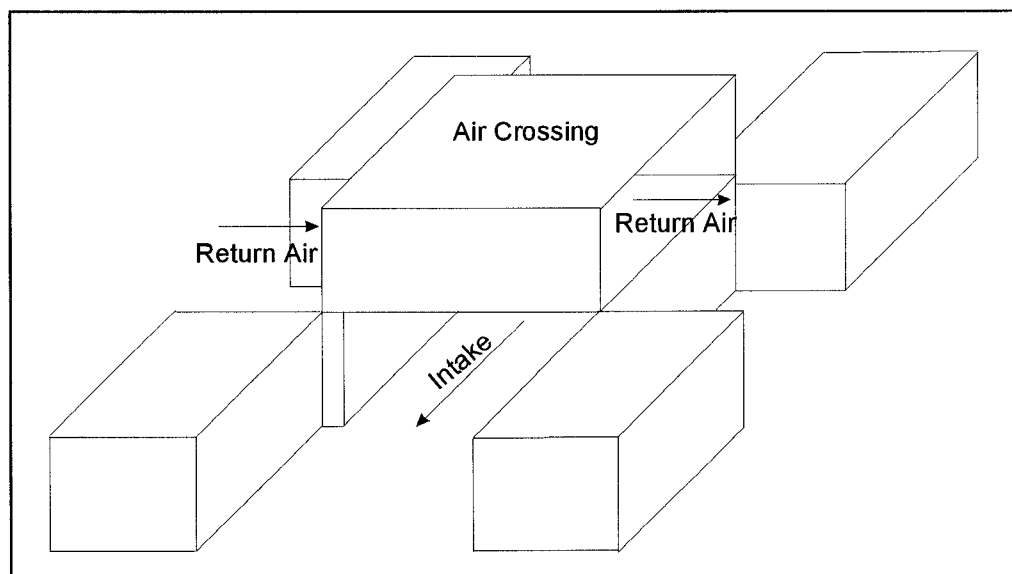

Figure 3.3.5: Sketch showing a typical design of an aircrossing with the intake and return airstreams crossing each other

50

- INTAKE AIR SIDE OF AIRCROSSING:- The aircrossings that were measured were situated in series with each other and considered for a single roadway only. The tests were carried out in such a manner that the resistance values can be given per crossing for ease of calculation as will be explained. The resistance increase per aircrossing is as follows:

$$R1 = 0,00128 \ Ns^2/m^8$$

$$R2 = 0,00256 \ Ns^2/m^8$$

$$R3 = 0,00512 \ Ns^2/m^8$$

$$R4 = 0,00528 \ Ns^2/m^8$$

$$R5 = 0,00640 \ Ns^2/m^8$$

The values as shown should then be used in the following manner:

1. Calculate the pressure loss for an open airway using Atkinson's formula

   Example:

   Area = 3,0 x 6,0 = 18 m^2

   Circumference = 2(3,0 +6,0) = 18 m

   Length of airway = 120 m

   Air quantity = 20,0 m^3/s

   Friction factor for a mechanical miner, medium seam intake airway = 0,0099 Ns^2/m^4

   Air density = 1,03 kg/m^3

   Pressure loss for the open airway = **7,86 Pa**

2. Calculate the additional pressure loss with four aircossings installed using the square law formula:

   $$P = RQ^2$$

   $$= 0,00528 \times 50^2$$

   Pressure loss = **13,2 Pa**

These calculations should then be performed for every roadway where aircrossings are to be installed and added to the total pressure for the system.

- RETURN AIR SIDE OF AIRCROSSING:- Measurements were again made to be able to provide a resistance value per aircrossing for a single roadway. The resistance values per aircrossing are significantly higher due to the amount of shock loss as a result of the specific design of the structure on the return air side. The values were calculated as follows:

$$R1 = 0,00352 \ Ns^2/m^8$$
$$R2 = 0,00704 \ Ns^2/m^8$$
$$R3 = 0,01056 \ Ns^2/m^8$$
$$R4 = 0,01408 \ Ns^2/m^8$$
$$R5 = 0,01760 \ Ns^2/m^8$$

These values are then used in the same manner as was explained in the previous example.

4 CFD Simulation Results

The use of CFD simulations are essential in this project mainly for two reasons. First underground observations must be evaluated for accuracy and reliability and then the CFD program can be used to complete the set of values by performing calculations for scenarios that are difficult and sometimes impossible to arrange underground.

The value and the reliability of the CFD results must first be proved and the correction factor between the experimental work and the CFD simulations must also be determined. This correction factor is then used to adjust future simulations to be more comparable with the underground situation. To be able to do this, two sets of underground situations were simulated and compared with the actual underground tests that were performed. The underground tests and measurements were first conducted and the default values and parameters were programmed into the CFD model. The calculations and results from the CFD model were compared and the differences noted.

Taking cognisance of the differences that occurred, different underground situations were simulated and the correction factor was applied to the CFD results. It can therefore be assumed that the CFD results that will be discussed are reliable and can be related to the physical underground situation. Again it must be emphasised that the values that have been measured underground as well as on the CFD model are only to be used for planning and experimental purposes as they represent in general conditions on South African coal mines.

4.1 CFD simulations - Phase 1

In the first phase, two underground scenarios were measured in detail and these two scenarios were then simulated in a CFD model. The underground parameters were used as the boundary conditions in the CFD model as accurately as possible. This would then ensure that the CFD results could be related to the actual underground situation.

4.1.1 Raise-bore shaft

The first scenario that was measured and compared was the empty raise bore shaft that has previously been discussed. The airflow characteristics of the shaft were physically measured underground and these exact parameters were programmed into the CFD model, without revealing the pressure loss, resistance and friction values that were calculated from the underground measurements.

The CFD model had to determine the actual airflow pattern down the shaft, the pressure distribution and the shock losses around the shaft collar. From this information the friction factor could be calculated. The main objective was to determine whether the CFD model could provide the same pressure loss down the shaft as was measured underground. The results proved to be very close and in fact the simulations provided more detailed information than was possible to measure physically. The reader is referred back to Figure 3.2.3 for a sketch of the vertical raise bore shaft together with all relevant information and parameters. During the underground survey it was possible to measure a pressure drop of 120 Pa for a distance of 134 m. Unfortunately it proved to be somewhat difficult to move the trailing hose to different positions in the shaft for additional pressure readings that could be compared with the CFD results.

The CFD model provided results that were calculated from the shaft collar to the actual bottom of the shaft; at the position where the experimental pressure drop was measured, at the bottom of the shaft, the CFD model calculated a pressure drop of 112 Pa. The CFD results are shown on Figure 4.1.1(a) (on the following page) which illustrates the dynamic pressure distribution from the shaft collar to the bottom of the shaft. The sketch also shows in detail the amount of pressure that is destroyed around the shaft collar. This experiment showed that the calculated value and the experimental value are within 7 % of each other. Colour contour lines that illustrate the airflow distribution through the shaft are shown in Figure 4.1.1(b) (on the following page). The airflow disturbance around the shaft collar is illustrated in the different colour contours that represent different air velocities. The contours also show the distribution of the air down the shaft.
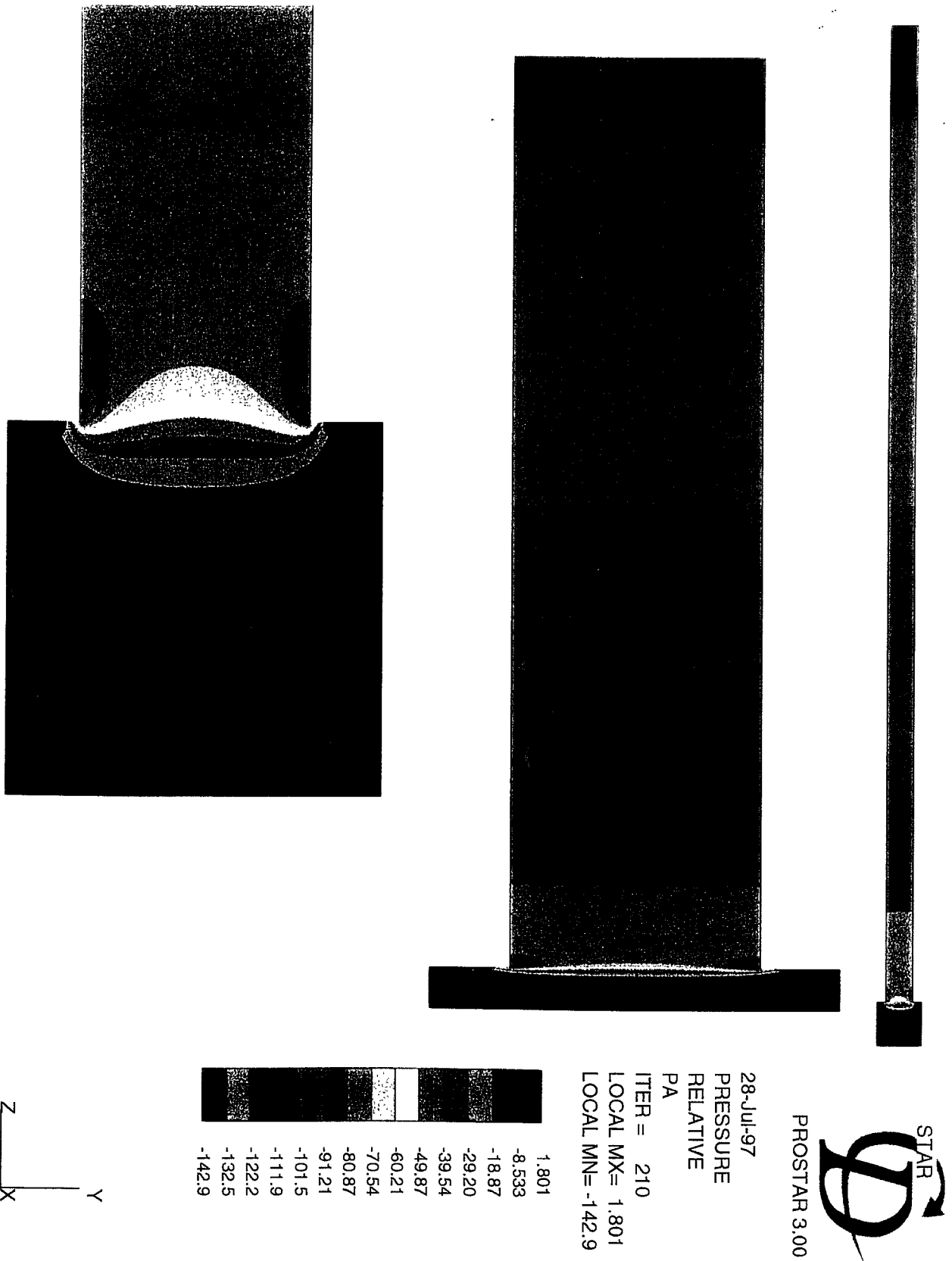
Figure 4.1.1(a): Colour contour lines that illustrates the pressure distribution down the downcast shaft
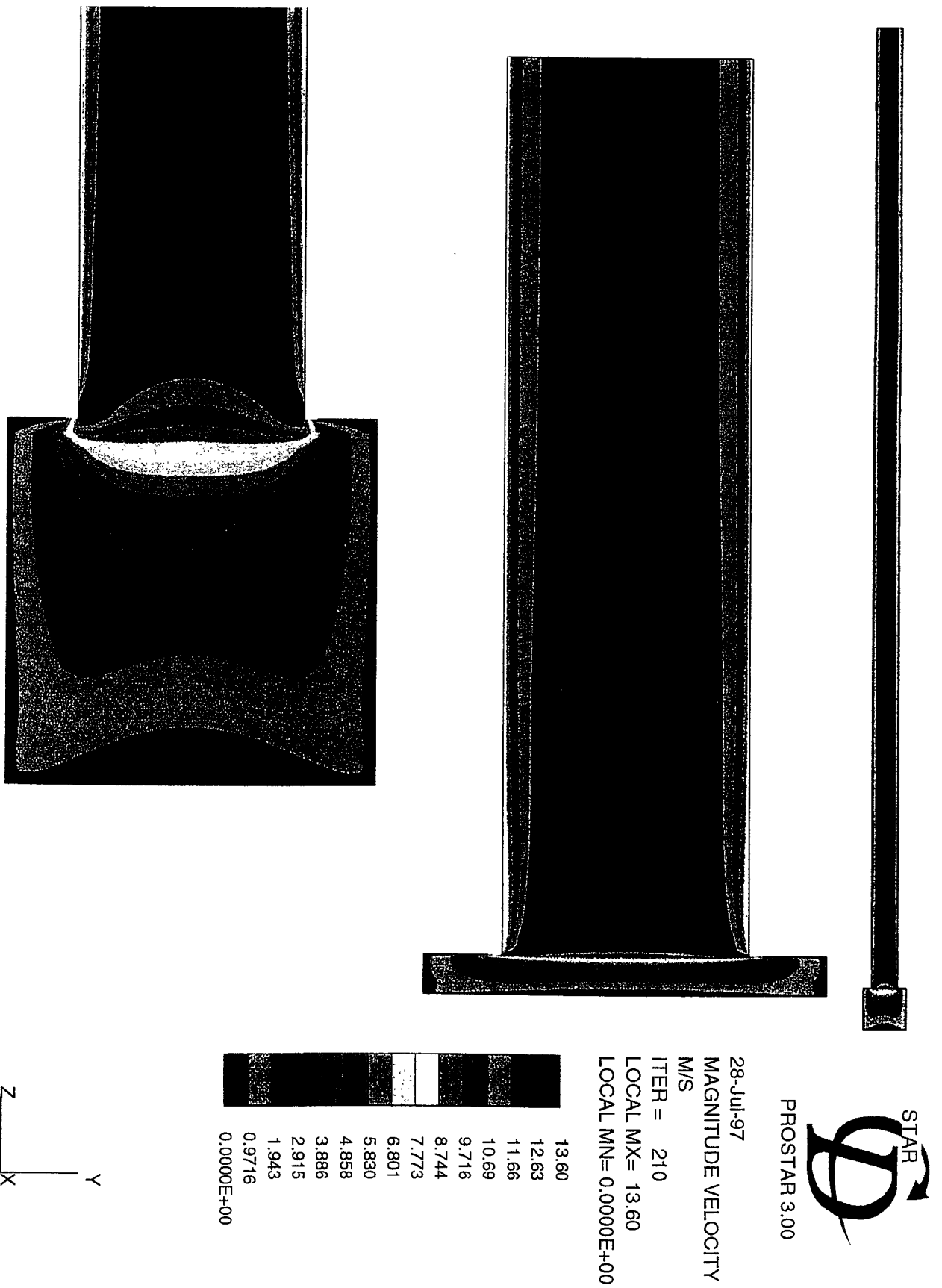
28-Jul-97
MAGNITUDE VELOCITY
M/S
ITER = 210
LOCAL MX= 13.60
LOCAL MN= 0.0000E+00

13.60
12.63
11.66
10.69
9.716
8.744
7.773
6.801
5.830
4.858
3.886
2.915
1.943
0.9716
0.0000E+00

PROSTAR 3.00

Figure 4.1.1(b): Colour contour lines that show the air velocity distribution down the downcast shaft

4.1.2 Single return airway: - underground measurements

In the second scenario, the airflow conditions in an underground single return airway were measured and the friction loss was calculated from the measurements. In contrast with the other scenarios that were discussed, special care was taken to record as much detail as possible that could be used as boundary conditions in the CFD model.

The total length of airway that was measured was 490 m. The airway consisted of side roads on both sides in which brattices and walls were installed. The airway parameters were extremely irregular and the walls were also installed at different distances from the airway. Fortunately the leakages through the walls and brattices could be kept to a minimum due to special preparation of the area before the test were performed. To be able to compare the underground results with the CFD simulation results, a number of pressure readings were taken at different distances with the use of the trailing hose and an electronic barometer. With all these pressure readings it would be possible to generate a graph of pressure against airway length which could then be compared directly with the results as calculated by the CFD model.

A total of eight readings were taken at 30 m intervals starting at 490 m and ending at 280 m. This means that pressure readings were taken over a total distance of 210 m, which was then also used in the CFD model, as it would be time consuming and expensive to model the full 490 m. Because of the total length of 490 m used underground, it was possible to record reliable pressure differences at these eight distances. The pressure readings at these positions will be shown together with the results as calculated by the CFD model for comparison purposes.

For determining the friction loss for this airway (which was developed by conventional means), the conditions at the 490 m position were recorded and were as follows:

- Roadway width = 7,8 m

- Roadway height = 3,69 m

- Air quantity = 64,47 m^3/s

- Airway length = 490 m

- Air temperature = 11,9/15,8 $^\circ$C

- Dry air density = 1,03 kg/m^3

- Pressure difference = 29,84 Pa

The friction loss calculated for this particular airway was **0,01771 Ns^2/m^4**

4.1.3 Single return airway: - CFD simulations results

As was mentioned before, the CFD model was only set up for the actual 210 m that was measured underground to be able to make direct comparisons between the results. Figure 4.1.3(a) shows the layout of the 210 m airway that was measured and simulated showing the irregular airway dimensions and the individual positions of the walls in the side roads. These airway parameters were taken directly from the mine survey plans and are therefore correct as shown on the sketch.
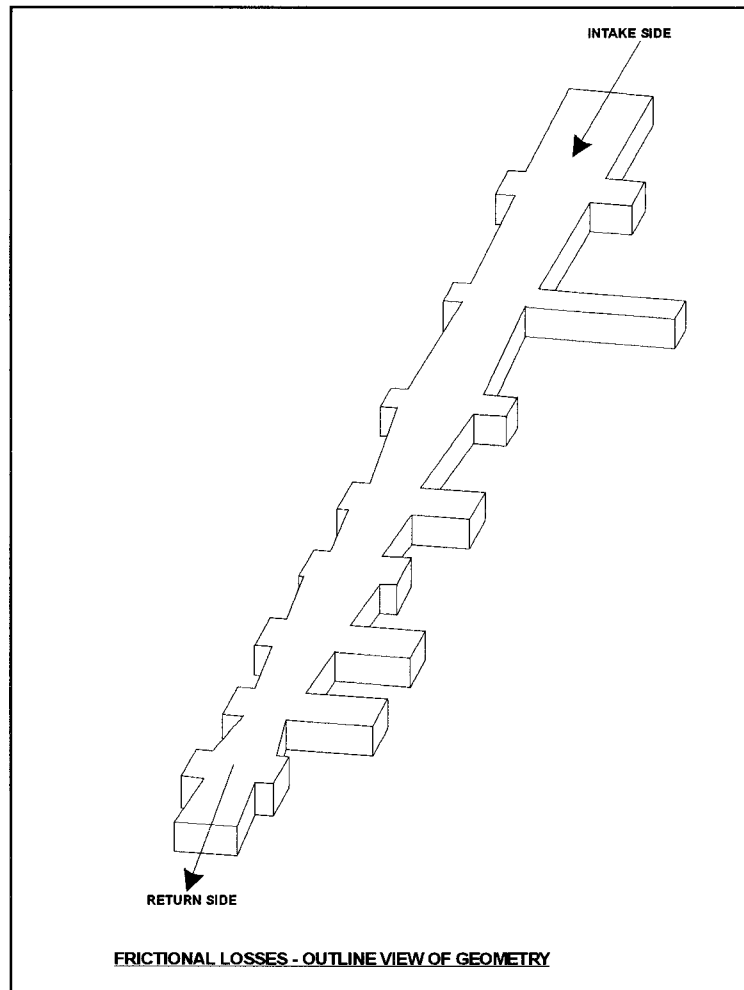

Figure 4.1.3(a): Sketch showing the layout of the single return airway

The following boundary conditions were used in the CFD model:

- Air quantity = 64,0 m³/s

- Dry density = 1,028 kg/m³

- Airway dimensions = 3,69 m x 7,8 m

- Airway length = 210 m

For the purpose of the CFD model, the starting position of the airway was taken at the 280 m position and therefore the pressure difference at this point was taken as zero. From here the CFD model performed the numerical calculation over the distance of 210 m and the results were recorded for every 30 m. Logically, the pressure difference would not be the same as the experimental data that was measured because of the difference in length.

To be able to compare the experimental and CFD results, the pressure difference measured underground was also reduced from the measured value at that position to zero at the starting position. All other experimental values at the following eight positions were theoretically reduced by the same amount. In this way an exact comparison could be made between the two experiments and the discrepancy in results determined.

Figure 4.1.3(b) shows a graph that demonstrates the difference in pressure readings at the eight different positions for the underground measurements and the CFD results.
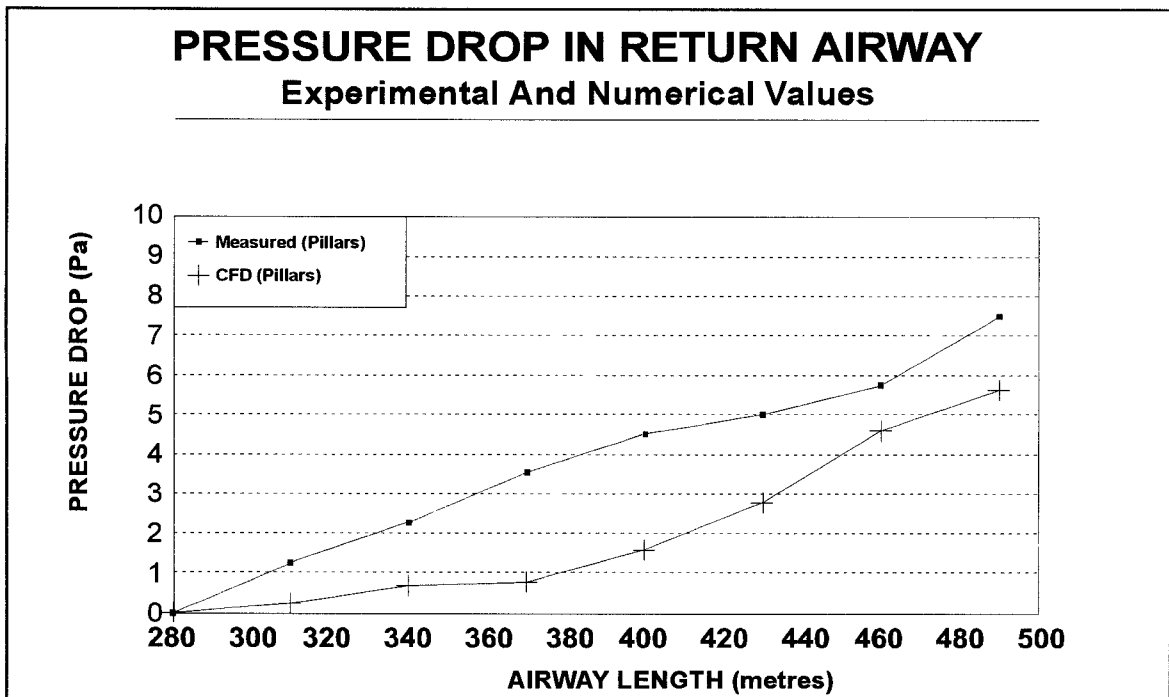

Figure 4.1.3(b): Graph showing the difference in pressure readings between CFD and underground measurements

Both the graphs commence at zero and end at the 210 m position. In between the two points, the graphs vary considerably in value but eventually end up fairly close together. The large variation in readings could be due to the sensitivity of the electronic manometer that was used and the human error that is always involved. The CFD model is more accurate in recognising the effect of the irregularities in the airway parameters as is clearly demonstrated in Figure 4.1.3(a).

What is important, however, is the difference in the values at the end of the graph. The measurement as would be taken underground at this position under these conditions is shown as being 7,5 Pa in comparison with the 5,6 Pa that was calculated by the CFD model. These values are within 10 % from each other, which proves that it is possible to use the CFD model to predict underground airflow behaviour when the boundary conditions are measured accurately.

It must be emphasised that this CFD model is by no means refined and in this case the corners of the pillars were taken as right angled and not round and rough as would be in the real situation. To obtain more reliability in these numerical values, a correction factor, as was determined with the two experiments described above, was built into the follow-up work that was conducted on the CFD model. Therefore the results can be related more accurately to the underground situation and predictions of airflow conditions and behaviour can be used with more confidence than in the past.

Figures 4.1.3(c) (on the following page) shows colour contours that demonstrate the airflow distribution through this airway and also show the conditions inside the side roads.

To determine the effect of the side roads on the overall pressure distribution and the pressure loss that occurs as a result of these developments, an additional simulation run was performed that only shows the full airway with the irregular dimensions, but without the side roads. The result is demonstrated in Figure 4.1.3(d) which graphically compare the two simulations.
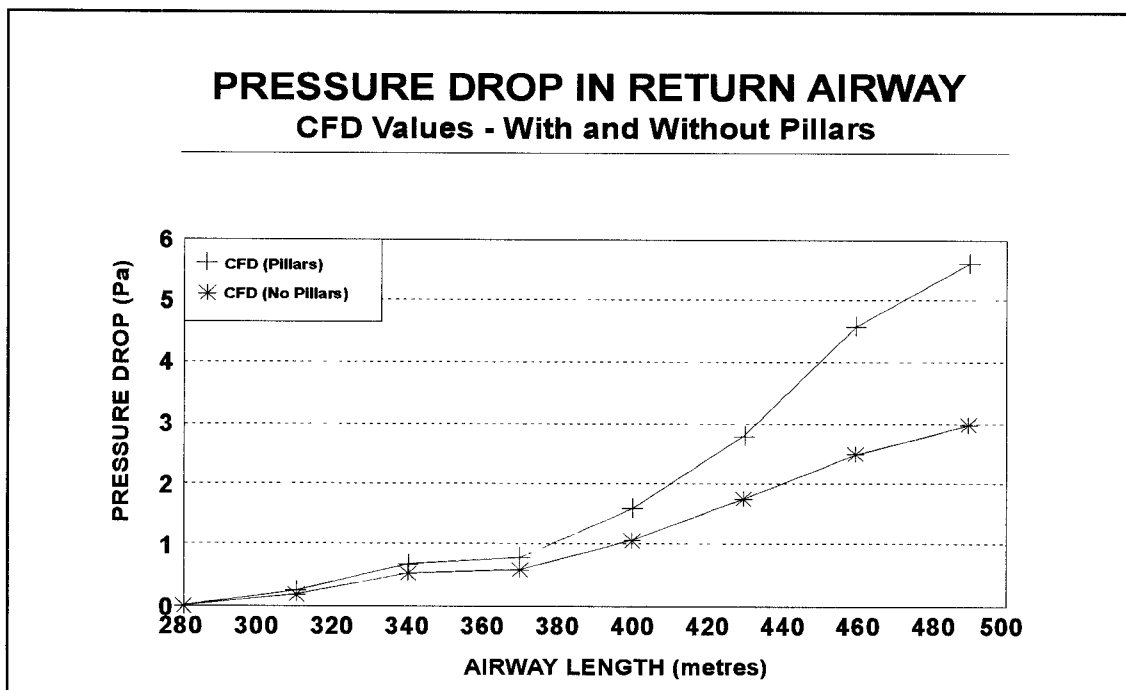

Figure 4.1.3(d): Graph showing the difference in pressure loss between an airway with and without side roads.

STAR

PROSTAR 3.00

08-Sep-97
MAGNITUDE VELOCITY
M/S
LOCAL MX= 4.386
LOCAL MN= 0.0000E+00

4.386
4.073
3.760
3.446
3.133
2.820
2.506
2.193
1.880
1.566
1.253
0.9399
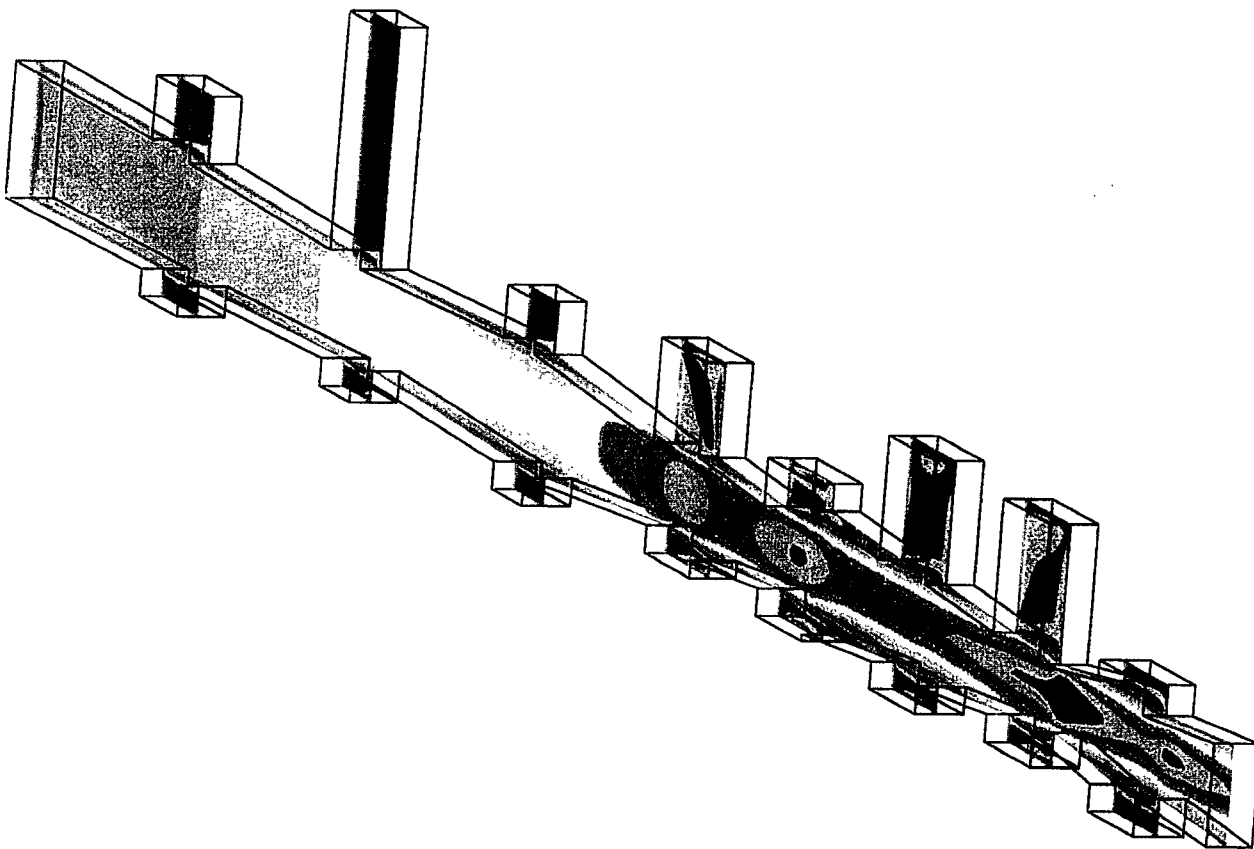0.6266
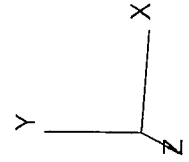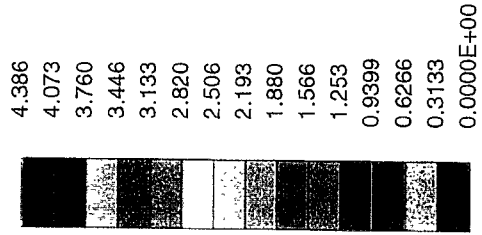0.3133
0.0000E+00

X
Y
Z

Figure 4.1.3(c): Colour contour lines that demonstrate the airflow distribution through the single return roadway with the side roads

60

To show the effect of an increase in air velocity on the overall pressure loss as a result of the shock losses and recirculation caused, it was decided to conduct an additional simulation run where the air velocity through this airway was increased to 5,0 m/s. The result was that an considerable increase in pressure loss occurred for this length of airway. This increase in pressure drop is demonstrated in Figure 4.1.3(e), which shows a graph that compares the pressure drop of the two velocity settings.
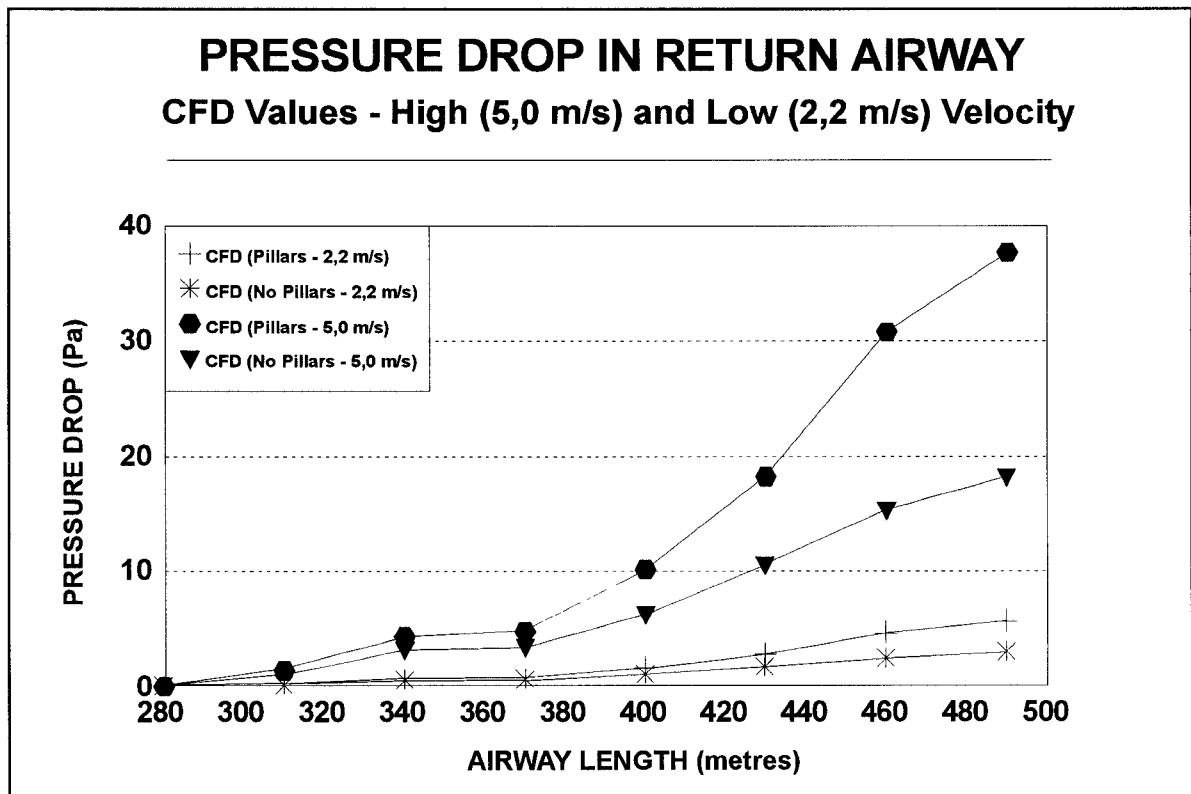

PRESSURE DROP IN RETURN AIRWAY
CFD Values - High (5,0 m/s) and Low (2,2 m/s) Velocity

Figure 4.1.3(e): Graph showing the difference in pressure loss for two velocity settings

4.2   CFD simulations - Phase 2

Under Phase 1, the objective was to establish the reliability of the CFD results and to determine the correction factor that should be used to calibrate the simulations to be more closer to underground measurements and conditions. This was done successfully and this correction factor was brought into consideration with the next set of CFD simulations that were performed.

In the next set of simulations, the same underground model was used to determine the effect of different conditions and parameters on the airflow behaviour and the pressure distribution profile. The following investigations were performed:

- To determine the effect of using round edges on the pillars instead of sharp edges.

- To determine the effect of different sidereal lengths on the total pressure loss.

- To determine the effect of different pillar lengths on the total pressure loss.

- To determine airflow behaviour within multiple roadways.

For these simulations, side roads were only simulated on the one side of the airway and not on both sides as before. All of these investigations were done using generic values and parameters that were measured underground for boundary conditions. The results that were obtained must be seen as general trends and airflow behaviour that could be used by the industry to better understand the effect of certain conditions in airflow and pressure loss. The information from these investigations can be used with confidence to make more educated decisions with regard to underground ventilation.

4.2.1 Sharp pillar edges vs Round pillar edges

To make the CFD simulation results more reliable and to create a better understanding of the effect of different pillar shapes on airflow, pressure loss and shock loss, it was decided to compare round and sharp edges when the same airflow conditions exist. In the model that was used, only three side roads on both sides of the airway were included in the model over a total length of 132 m. The width of the side roads was kept at a constant of 6,6 m and the road height at 3,7 m. The air quantities were kept the same as described in Phase 1. The side roads on the one side of the airway were kept constant at 2,0 m in depth while the side roads on the opposite side varied in depth. The radius for the round edges was kept constant at 0,5 m. Figure 4.2.1(a) shows a layout of the airway and side roads as they were simulated.
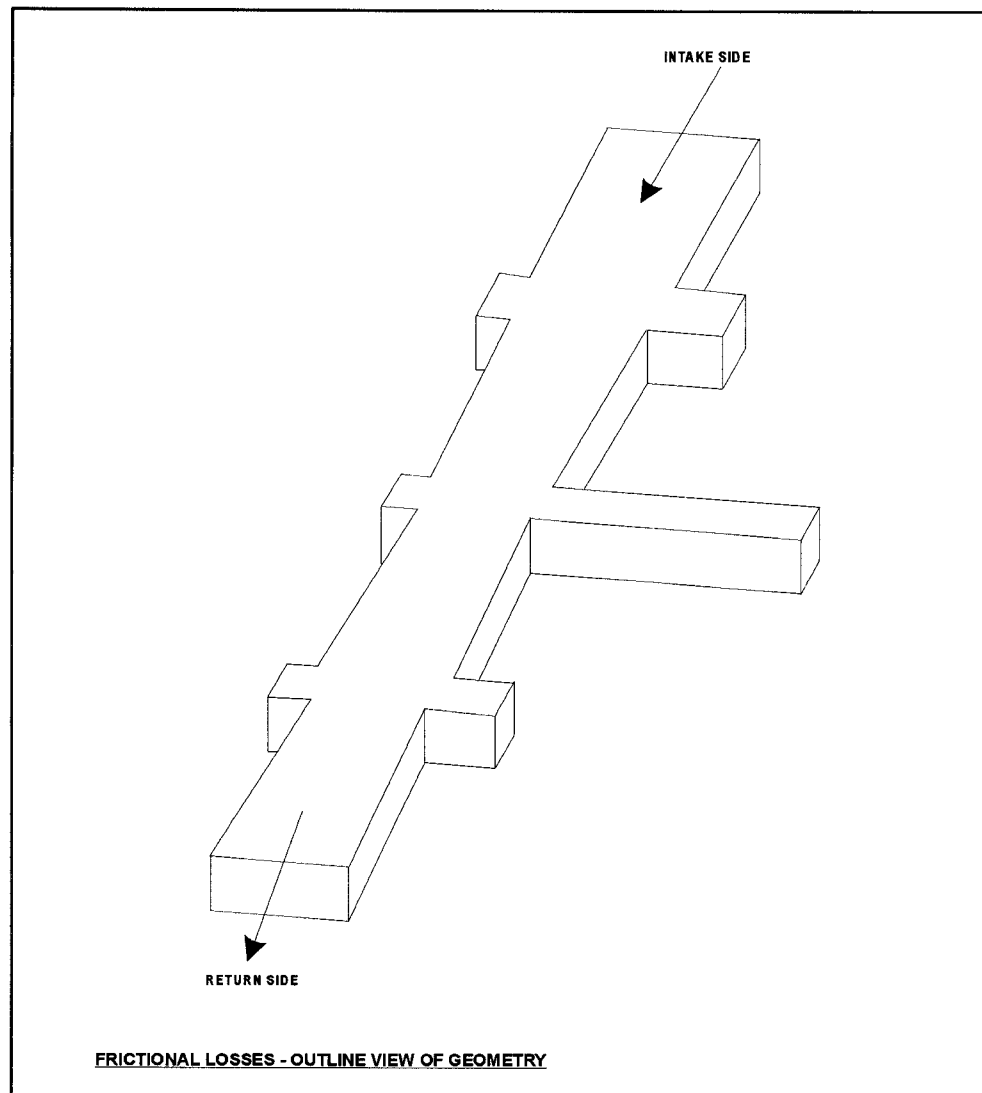
INTAKE SIDE

RETURN SIDE

FRICTIONAL LOSSES - OUTLINE VIEW OF GEOMETRY

Figure 4.2.1(a): Sketch showing the layout of the model used for comparing pillars with sharp and round edges.

For this experiment, three situations were simulated. As a reference case, the airway was simulated without any side roads, followed by side roads with sharp edges and then pillars with round edges. The results of this experiment are shown in Figure 4.2.1(b), which graphically compares the difference in pressure losses for the three scenarios.
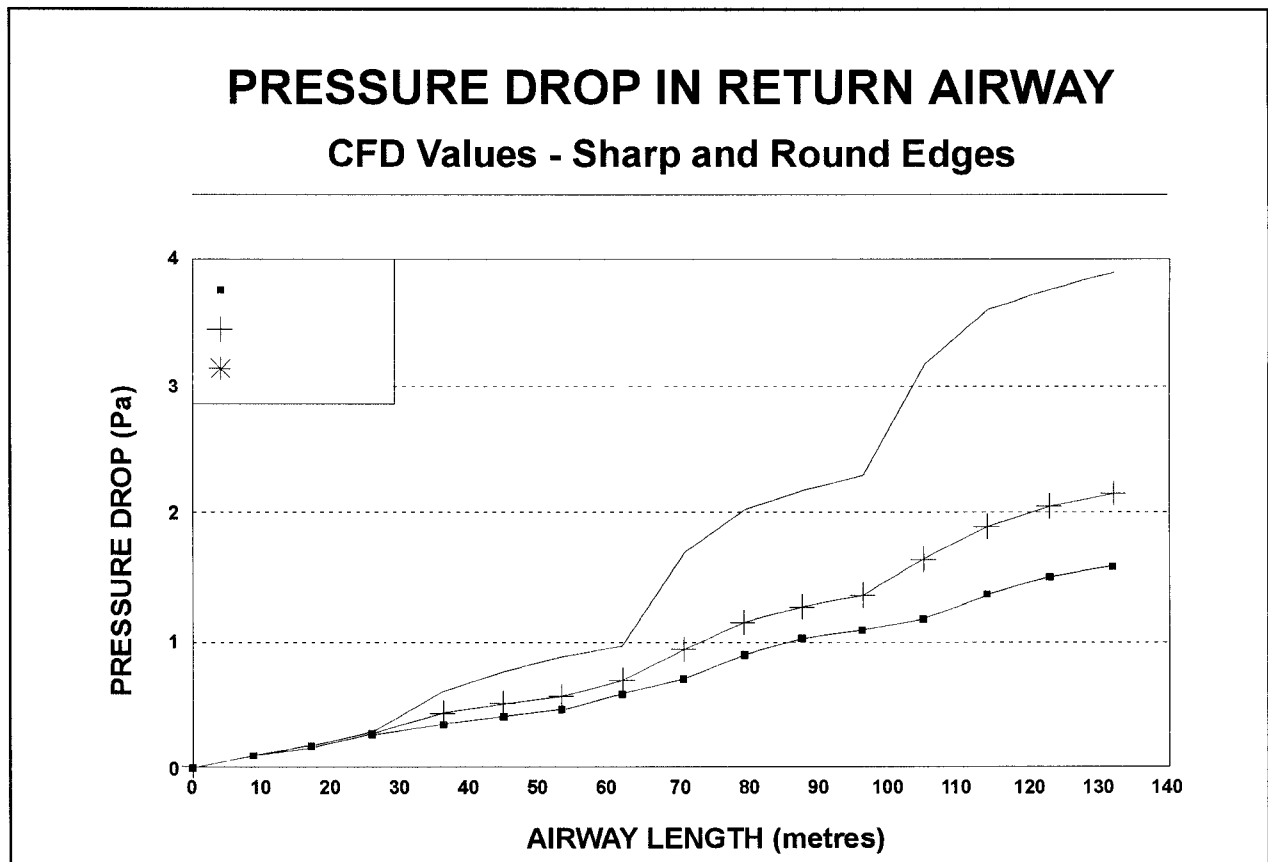
63

PRESSURE DROP IN RETURN AIRWAY

CFD Values - Sharp and Round Edges

Figure 4.2.1(b): Graph showing the comparison between no side roads, side roads with sharp edges and side roads with round edges.

The graph shows that more pressure is lost when the pillars are mined with round edges than would be the case when the edges were sharp. The reason for this is that the round edges facilitate more the flow of air and that the air penetrates deeper into the side road. More pressure is therefore destroyed as a result of this. This phenomenon is clearly demonstrated in Figures 4.2.1(c) and 4.2.1(d) (on the following pages). These sketches show the difference in the airflow patterns when flowing past a sharp corner and when flowing past a round corner respectively.

4.2.2 Variation in the side road lengths

The reason for simulating different side road lengths, was to provide an estimate on the optimum position of a wall or stopping with regard to the total pressure loss. For this exercise, five side roads were simulated with the pillar lengths set at 20 m, the individual roadway width was 6,6 m and the seam height set at 3,7 m. Following the results from the previous section, it was decided to keep the edges at a radius of 0,5 m. The total length of roadway was simulated at 142,2 m.
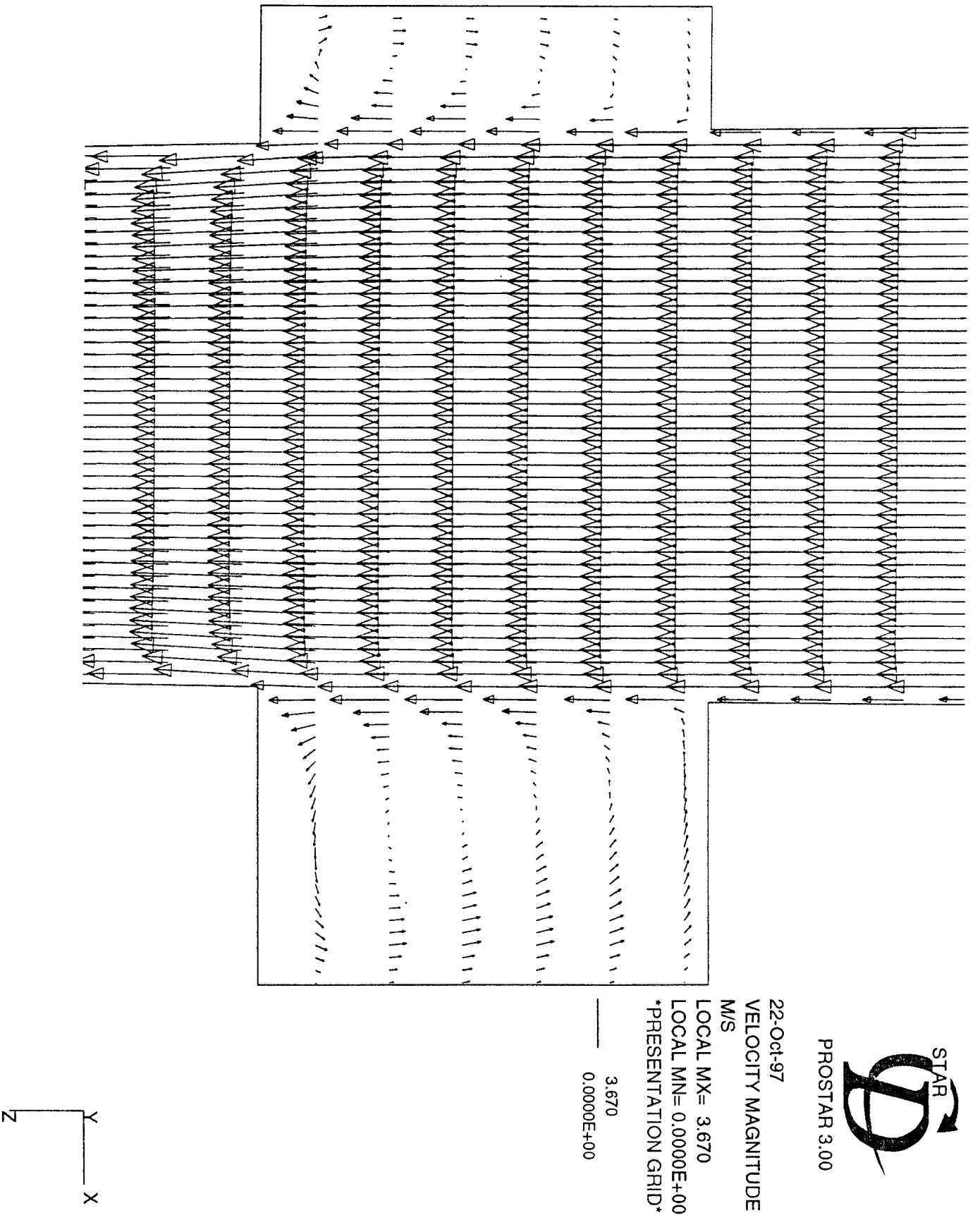
Figure 4.2.1(c): Velocity vectors demonstrating the behaviour of air when flowing past a pillar with sharp corners

PROSTAR 3.00

22-Oct-97
VELOCITY MAGNITUDE
M/S
LOCAL MX= 3.670
LOCAL MN= 0.0000E+00
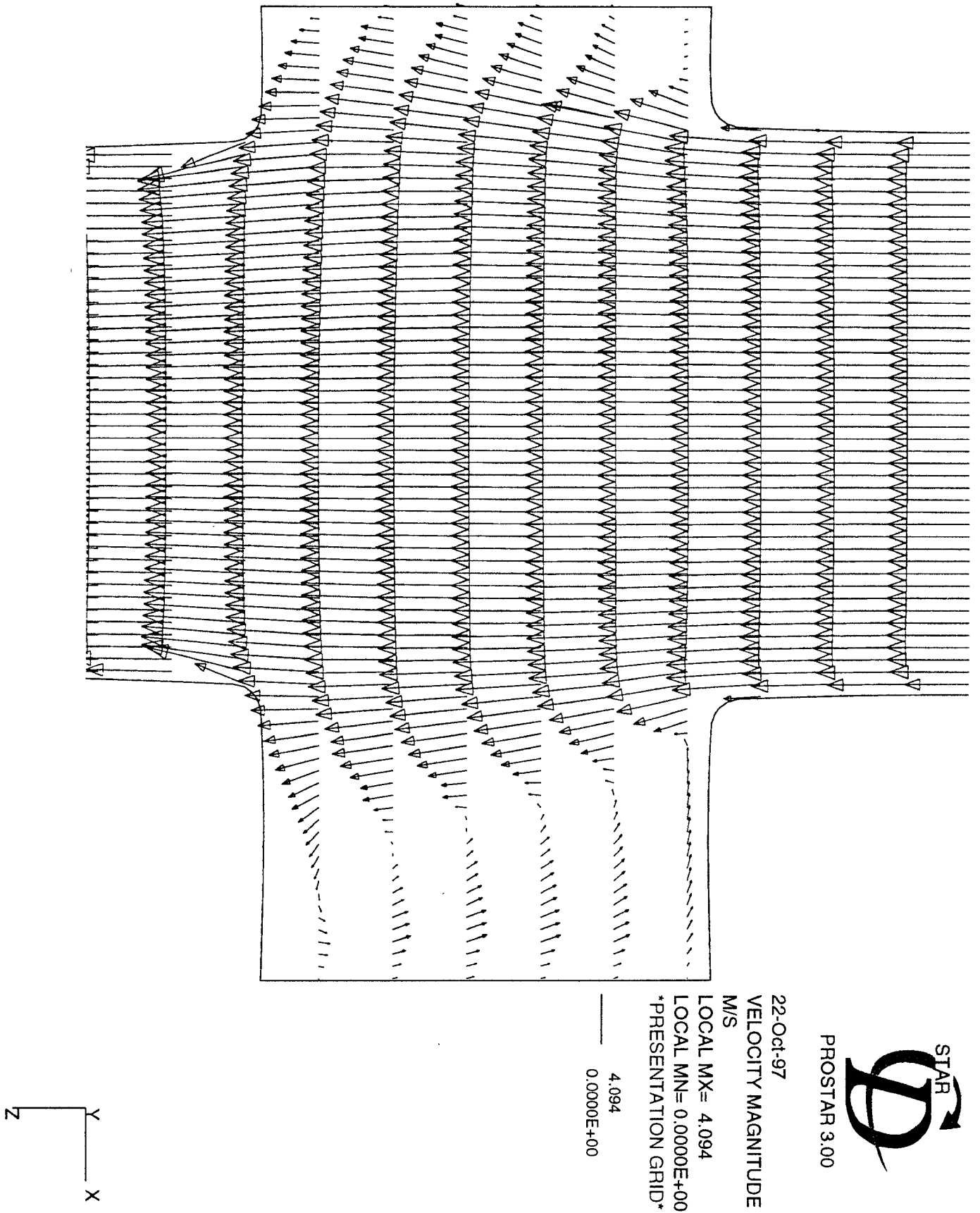*PRESENTATION GRID*

3.670
0.0000E+00

Figure 4.2.1(d): Velocity vectors demonstrating the behaviour of air when flowing past a pillar with rounded corners

The side road depths were simulated at 1,0 m, 3,0 m and 5,0 m from the airway. Again the results were compared with a reference case where no side roads were present.

Figure 4.2.2(a) shows a graph where the four scenarios are compared with regard to the total pressure loss over the full length of the airway.
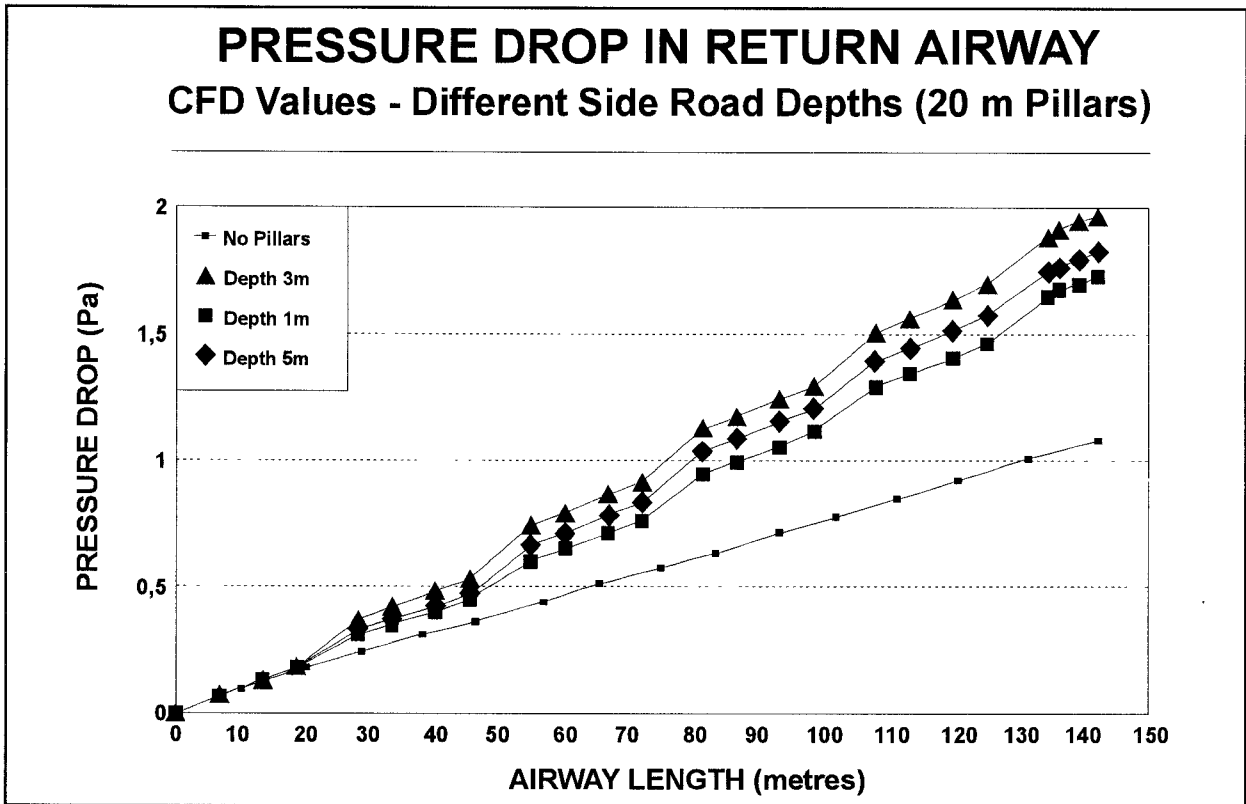

PRESSURE DROP IN RETURN AIRWAY
CFD Values - Different Side Road Depths (20 m Pillars)

Figure 4.2.2(a): Graph showing the difference in total pressure drop when the side roads are developed at different lengths from the airway.

The condition with the least resistance and shock loss is indeed the airway with no side roads followed by the scenario where the side roads were developed at 1,0 m from the airway. Interestingly enough, the 3,0 m development shows a higher pressure drop than the 5,0 m development. This indicates that the total pressure loss reaches a maximum at a distance of approximately 3,0 m, which is due to the recirculation pattern of the air inside this sideroad. These findings confirm previous research findings on the effect of airflow on empty headings (Meyer,1991)[18]. When a curve fitting is performed on this data, the following expression is obtained:

$$\Delta P = -0,01315.L^2 + 0,08589.L + 0,082307$$

where L is the depth of the side road. In this case it can then be calculated that the maximum pressure will be at a side road of 3,27 m.

This curve is demonstrated in Figure 4.2.2(b), which shows the side road lengths vs the total pressure loss per side road. For all practical purposes it can be assumed that the maximum pressure loss will occur when a side road is closed off at 3,0 m depth. This value is then used as the worst case scenario for all other calculations that follows.
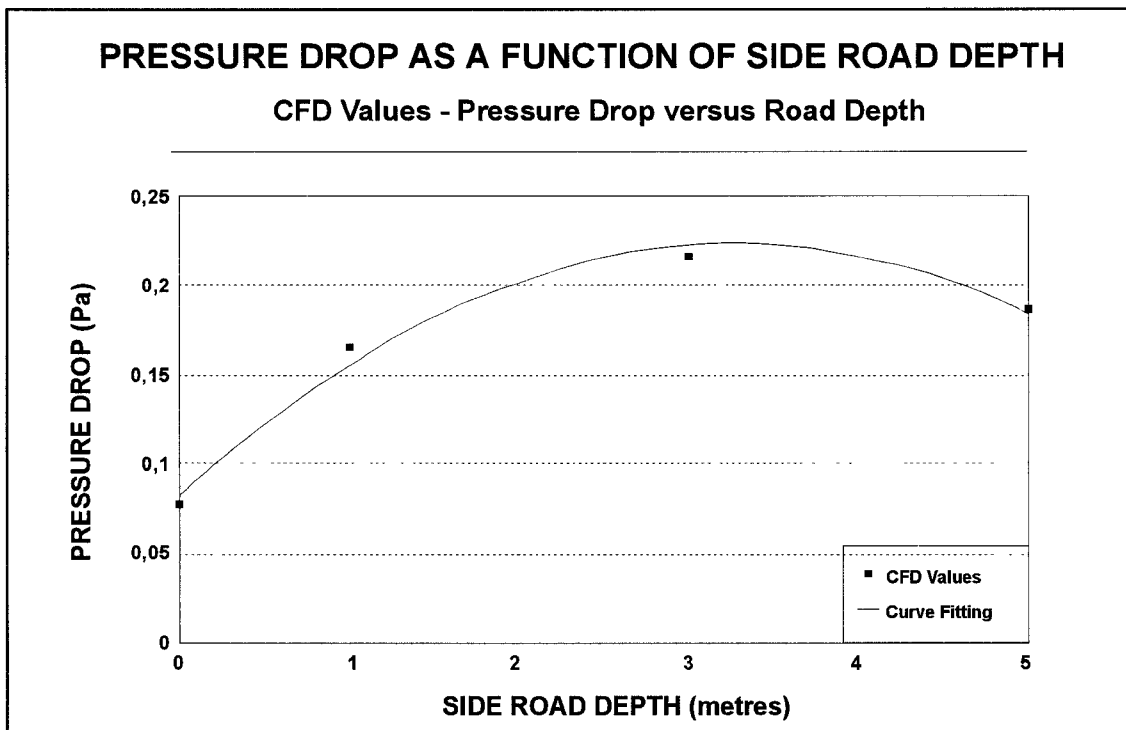

PRESSURE DROP AS A FUNCTION OF SIDE ROAD DEPTH
CFD Values - Pressure Drop versus Road Depth

Figure 4.2.2(b): Graph showing the pressure drop as a function of the side road depth.

4.2.3 Variation in pillar lengths (number of side roads)

This exercise was done to determine a pressure loss or shock loss value that can be used per pillar for planning purposes. For this simulation, a number of different pillar lengths, varying between 12 m, 20 m and 30 m, were used. Following the results from the previous exercise, the side road lengths were set at 3,0 m, which is where the highest pressure loss occurs. The side roads were set at 6,6 m width and 3,7 m height. The total length of airway was kept at 142,2 m. Two reference cases were included in the simulations. The airway was again simulated without any side roads and the 30 m scenario was repeated with sharp edged pillars. Figure 4.2.3 shows the results in the form of a graph where the five sets of results are compared with each other.
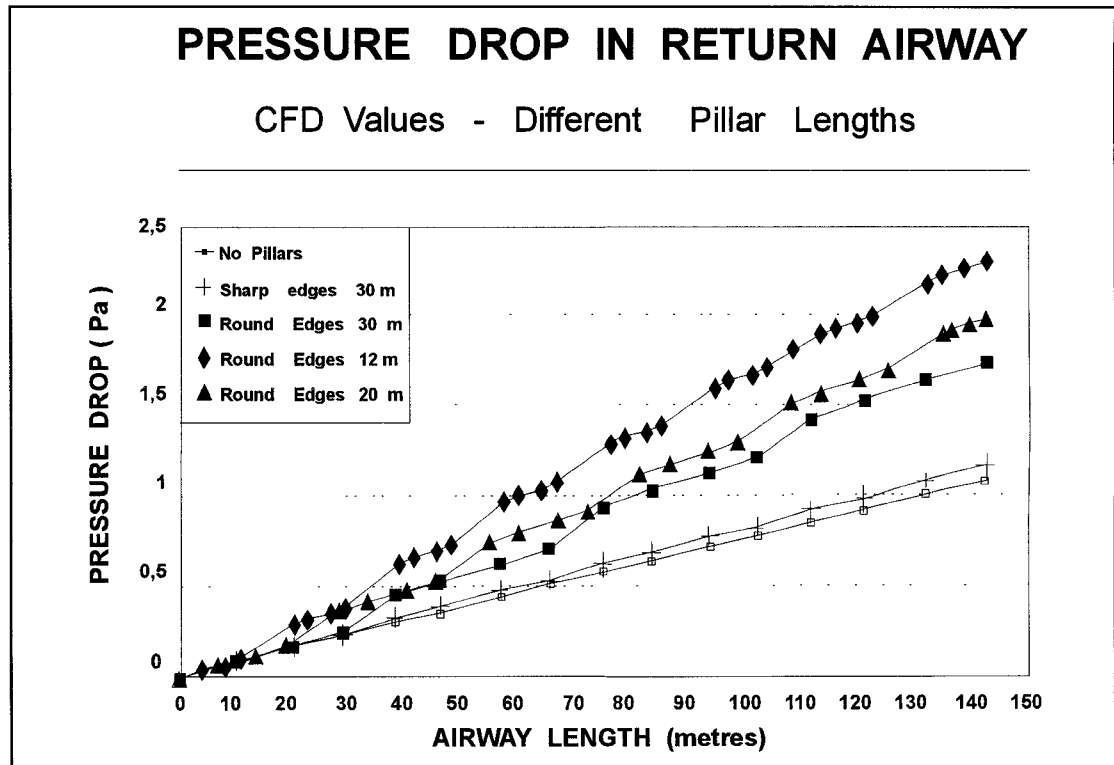
PRESSURE DROP IN RETURN AIRWAY

CFD Values - Different Pillar Lengths

Legend:
- No Pillars
- Sharp edges 30 m
- Round Edges 30 m
- Round Edges 12 m
- Round Edges 20 m

Y-axis: PRESSURE DROP (Pa)
X-axis: AIRWAY LENGTH (metres)

Figure 4.2.3: Graph showing the results of the total pressure loss as a function of the different pillar lengths.

As is seen from the graph, the total pressure loss increases as the number of side roads increases or as the pillar lengths shorten as a result of the increased shock loss. Again it is shown that the sharp edged pillar creates less pressure loss than the round edged pillar

In order to calculate the pressure loss that a side road causes, a curve fitting was firstly performed on the data for the pressure loss in a roadway without any side roads. This led to the expression:

$$\Delta P_{wall} = 0,008196974.Z$$

where Z is the length of the airway in question. This expression was used to calculate the corresponding pressure loss for a length of roadway corresponding to the total sum of pillar length. In this way the pressure loss for the side roads could be calculated, as well as the pressure loss for each roadway. The data was used to perform a curve fitting to calculate the pressure loss as a function of the number of 6,6 m side roads. This led to the following expression:

$$\Delta P_{side\ roads} = 0,2147432.N$$

where N is the number of side roads. This gives the average pressure loss of 0,215 Pa per 6,6 m side road developed to 3 m depth. By using the above two expressions, the total pressure loss for any number of pillars (varying length) plus the pressure loss for any number of 6,6 m side roads of 3 m depth can be calculated.

69

At this point it must be stressed that the above expressions and results are only valid for the particular conditions and boundary conditions that were used. Any change in the airway dimensions, airway lengths, air velocity and/or pressure loss will result in different solutions. For other situations the values must be scaled using the correct expressions from the Atkinson's Formula, as is explained below.

Throughout the report, use was made of the Atkinson's Formula (combination of equations 1 and 6) to calculate the pressure losses and the K-factors.

From the Atkinson's Formula, it can be seen that:

$$\Delta P \propto C;$$

$$\Delta P \propto L;$$

$$\Delta P \propto V^2 ;$$

$$\Delta P \propto 1/A;$$

$$\Delta P \propto w$$

This implies that whenever a pressure drop has been calculated for a certain airway length L, the change in pressure loss for a new L can be calculated by using the following:

$$\Delta P_{new} = \Delta P_{old} \times L_{new} / L_{old}$$

The same procedure can be followed for changes in air density, air velocity, circumference and cross-sectional area.

4.3 CFD simulations - Phase 3

In this final phase of the project on k-factors, a three road situation was simulated to gain more knowledge on the behaviour of air and pressure in a multiroad situation. This must be seen as the first stage of a full scale project that should be considered in future on multiroad development and the effect of different parameters on the airflow behaviour in these situations. As was seen in the previous discussions, any change in the parameters causes a change in the pressure distribution and airflow behaviour. These simulations have been conducted using an idealised situation where regular dimensions were used throughout.

The total length of the section was 142,2 m with an average roadway width of 6,6 m and a seam height of 3,7 m. The side roads were 10,0 m long between the airways. An average air velocity of 2,315 m/s was introduced simultaneously into the three roads. The CFD model was then allowed to calculate and simulate the airflow and pressure distribution through the section. The layout of this section is shown in Figure 4.3(a).
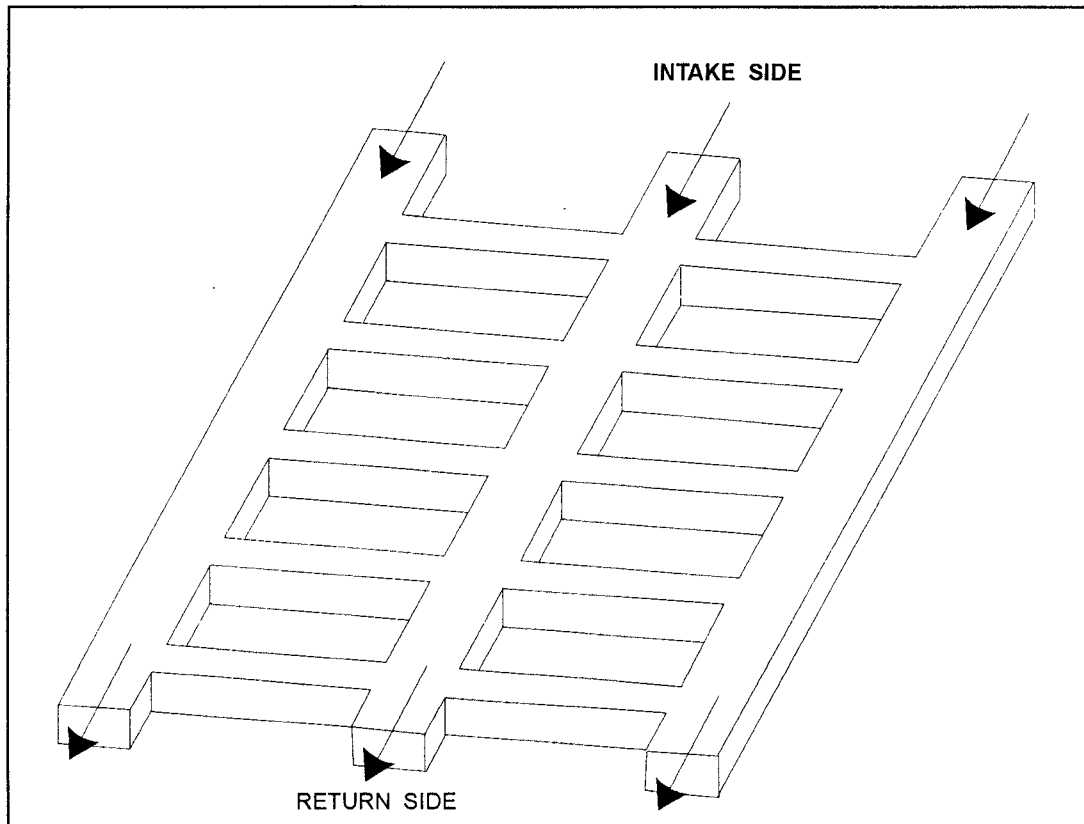

Figure 4.3(a): Sketch showing the layout of the section used for the multiroad simulations.

From the results it is shown that the air distributes fairly evenly through the section and that very *little* airflow is detected in the side roads. When looking at the colour contours representing the pressure distribution through the three roads, which can be seen in Figure 4.3(b) on the following page, the contours show that the pressure difference inside the side roads decreases from the point of intake towards the exit position. This means that little or no airflow will occur inside these side roads. Inside the three airways, the pressure loss increases from the point of intake towards the point of exit. This is due to the shock losses occurring at the corners of the pillars, which in this case were simulated to be sharp corners.

When looking at the airflow behaviour inside these three roads, the airflow vectors as shown on Figure 4.3(c) on the following page show that recirculation patterns are forming inside the side roads. These recirculation patterns prevent positive airflow inside these side roads and also contributed to the increase in the pressure loss. The colour contours that represent the air velocity contours inside the airways show that the airflow is evenly distributed through the three airways and that virtually no airflow is present inside the side roads. The air velocity inside the three airways is shown to be increasing towards the middle of the road from the intake side to the return side, while the air velocities against the sides are decreasing. This is due to the velocity pressure that is destroyed as the air rubs against the surface and as the difference in pressure gets less. These contours are shown on Figure 4.3(d) on the following page.

Figure 4.3(e) on the following page shows the airflow through the three airways and side roads in the form of airflow vectors. This again shows the lack of airflow inside the side roads.
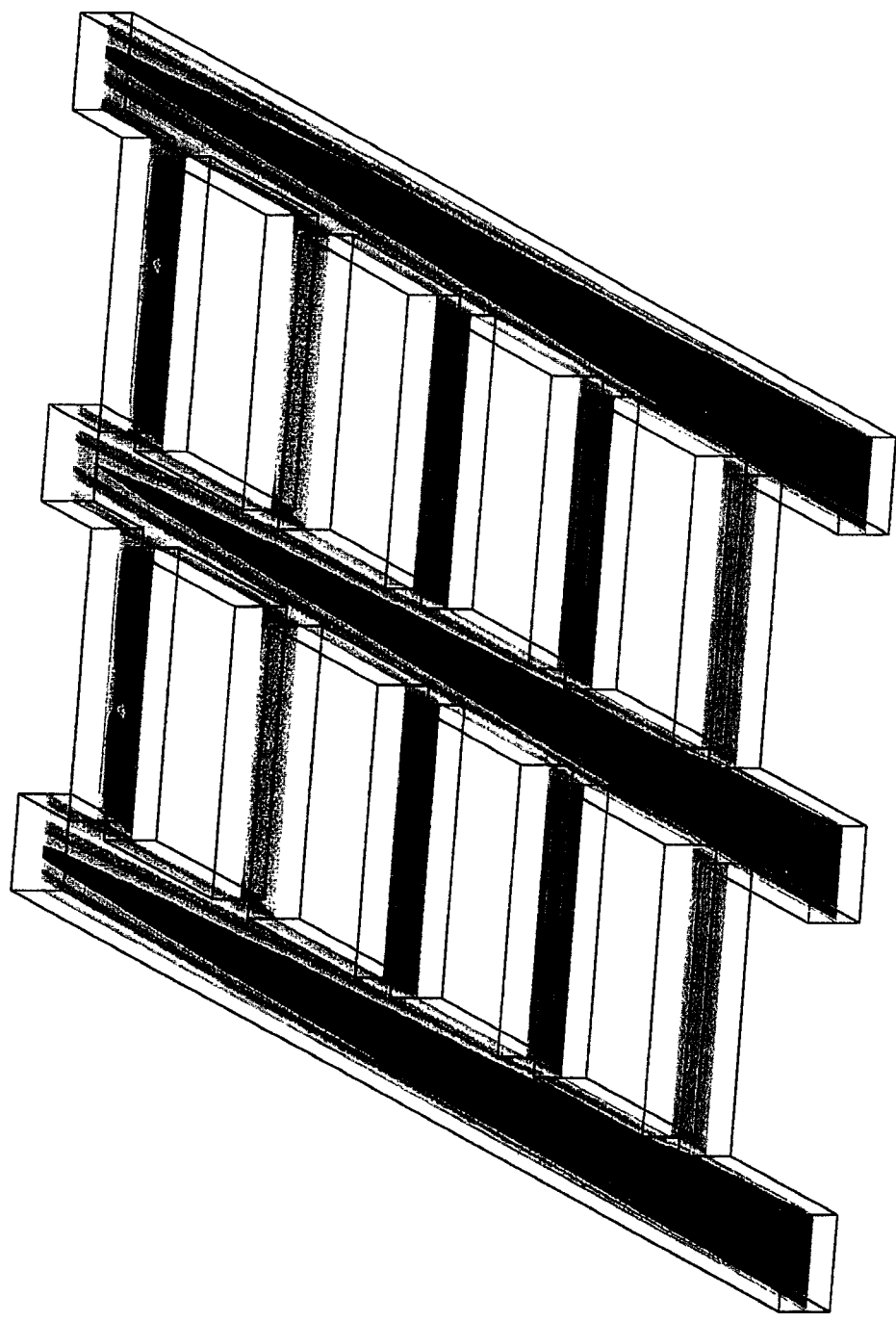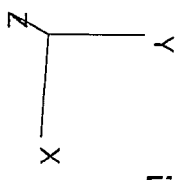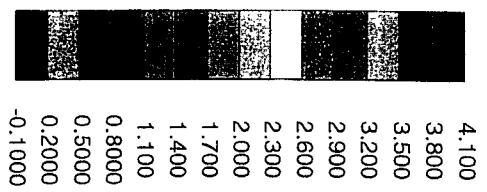
Figure 4.3(b): Colour contours showing the pressure distribution through the three roadways
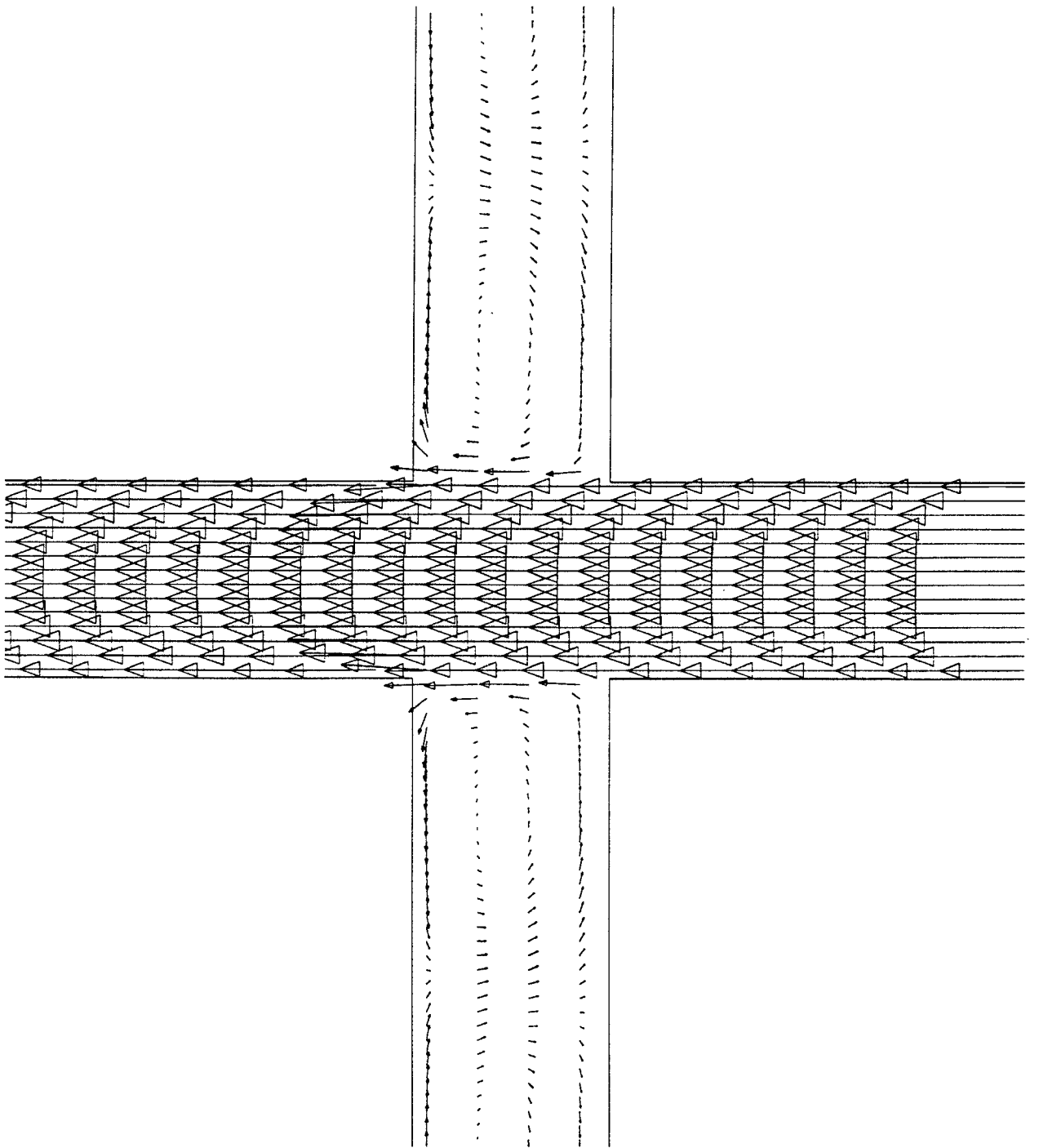
Figure 4.3(c): Velocity vectors demonstrating the recirculation patterns
that occur inside the side roads.

2.800
2.600
2.400
2.200
2.000
1.800
1.600
1.400
1.200
1.000
0.8000
0.6000
0.4000
0.2000
0.0000E+00
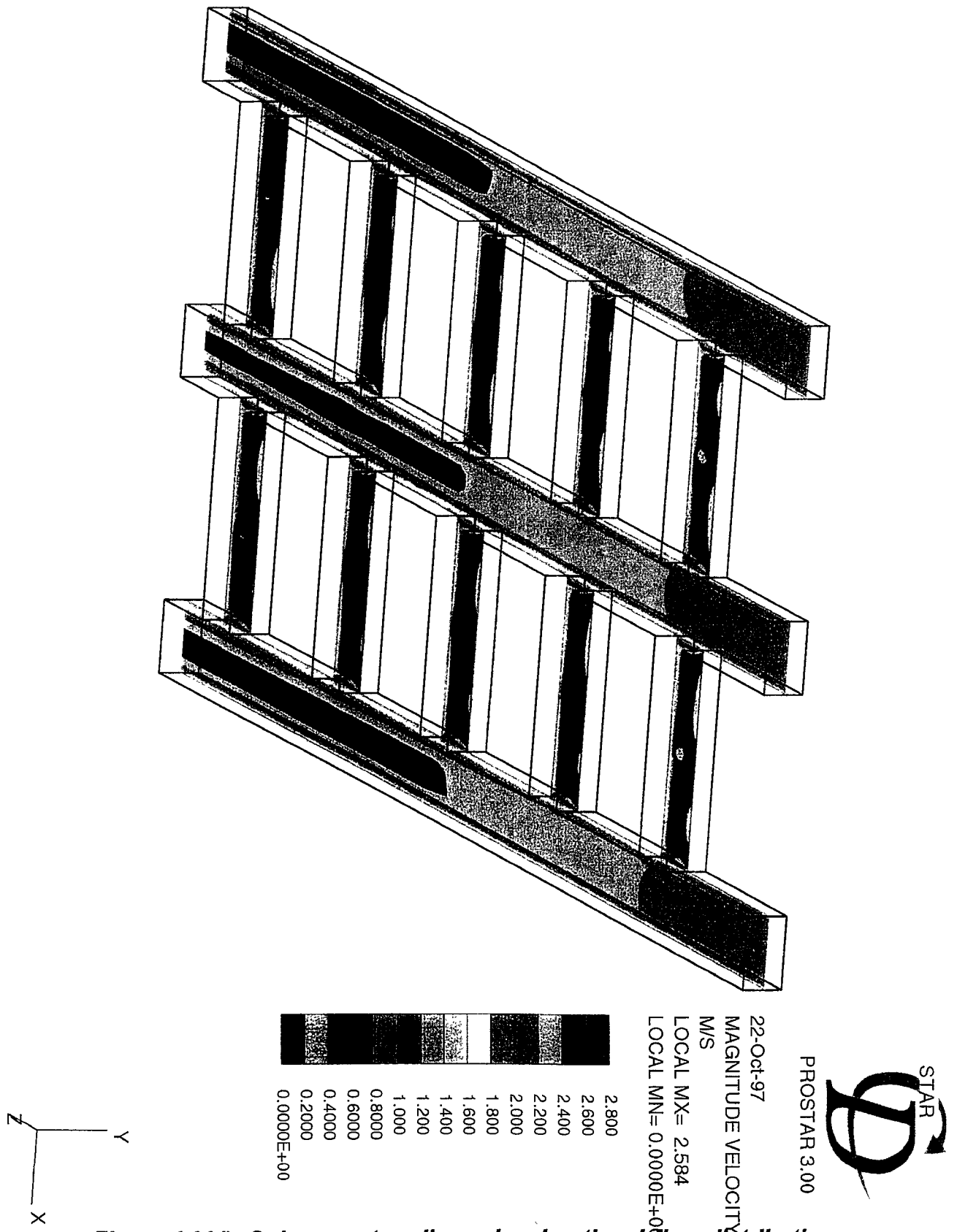
Figure 4.3(d): Colour contour lines showing the airflow distribution and behaviour through the three roadways
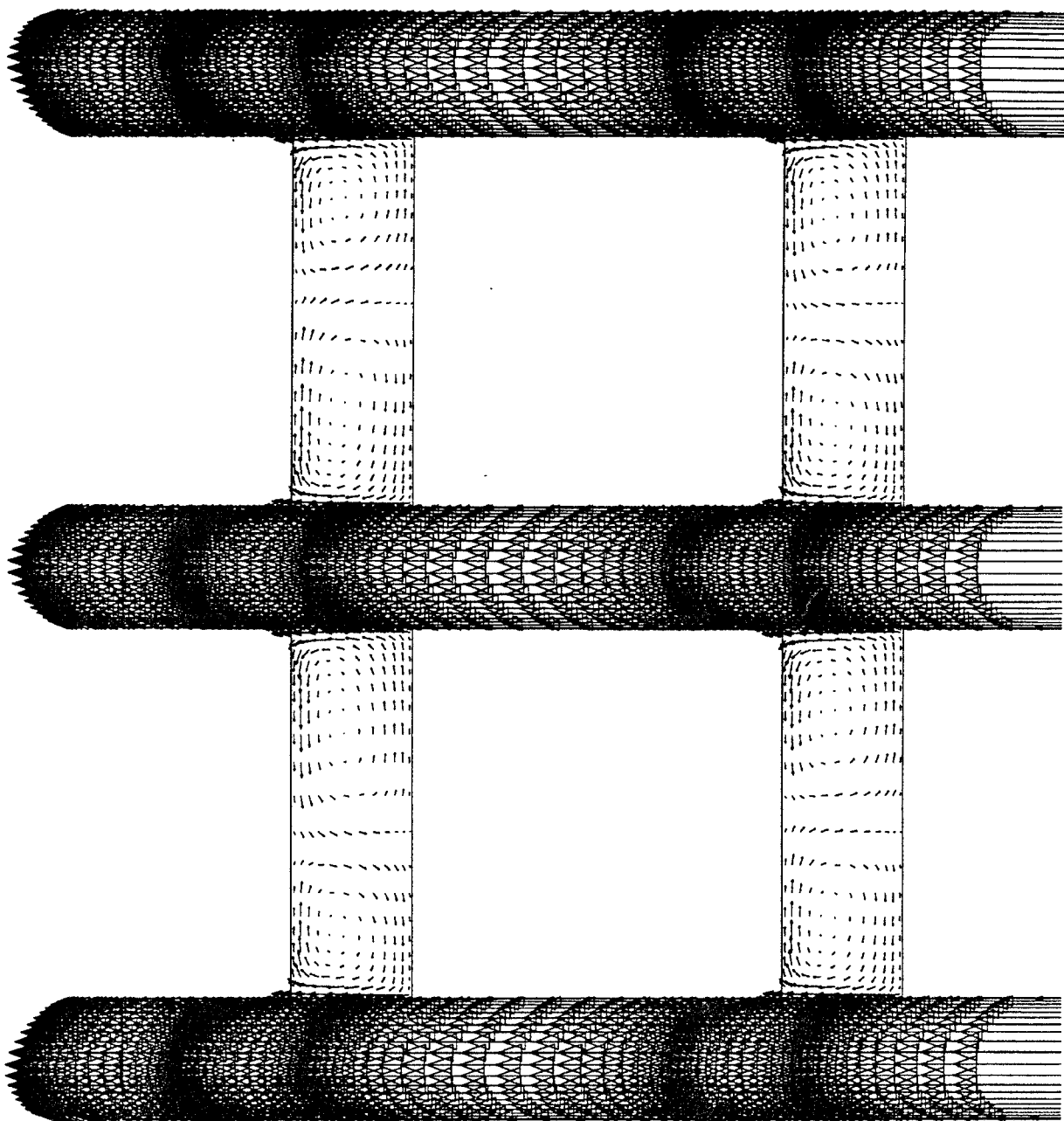
Figure 4.3(e): Velocity vectors showing the full airflow pattern throughout the three roadways and side roads

5 Concluding Remarks

At the end of this project, it may first of all be necessary to compare the results that were obtained from the different simulations that were performed with regard to pressure difference and friction factors that were calculated. The purpose would be to stress the fact that the friction factors for one road and for multiple roads would not differ considerably and that the pressure differences would also be close to one another.
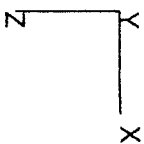
Before the comparison can be made, it is necessary to take note again of all the scenarios that were simulated. Table 5(a) summarise the different phases of the CFD simulations.

Table 5(a): Summary of the different scenarios that were simulated.

PHASE 1	
Phase 1.1	Single return airway with side roads (one side 2,0 m, other side varying). Sharp edges
Phase 1.2	As 1.1, but with round edges
Phase 1.3	Single return airway with no side roads
PHASE 2	
Phase 2.1	Single return airway with 30 m pillars; sharp edges, 3 m side roads
Phase 2.2	Single return airway with no side roads
Phase 2.3	Single return airway with 30 m pillars; round edges, 3 m side roads
Phase 2.4	Single return airway with 12 m pillars; round edges, 3 m side roads
Phase 2.5	Single return airway with 20 m pillars; round edges, 3 m side roads
Phase 2.6	Single return airway with 20 m pillars; round edges, 1 m side roads
Phase 2.7	Single return airway with 20 m pillars; round edges; 5 m side roads
PHASE 3	
Phase 3.1	Multiple roadways with 20 m pillars; sharp edges, 10 m side roads

With the use of the above reference system, a summary of the results can be presented as follows:

Table 5(b) shows the pressure differences that were calculated by the CFD model for the various scenarios that were simulated, together with the k-factors that were calculated. It is important to also note the effect that round and sharp corners of pillars have on the total pressure loss.

Note must be taken that the k-factors and pressure losses that are displayed are purely numerical and should not be related directly to the underground situation without recognising the specific conditions and parameters under which these calculations were performed. They are only displayed for comparison purposes in order to demonstrate the effect of different conditions and parameters on pressure and friction-factors.

Table 5(b): Summary of the various friction factors and pressure losses determined for the different scenarios investigated

	ΔP (Pa)	K-factor (Ns^2/m^4)
Phase 1.1 (Sharp edges)	2,128	0,0043
Phase 1.2 (Round edges)	3,879	0,0079
Phase 1.3 (No pillars)	1,559	0,0032
Phase 2.1 (Sharp edges)	1,155	0,0028
Phase 2.2 (No pillars)	1,072	0,0026
Phase 2.3 (3 pillars, 30 m, 3 m depth)	1,717	0,0042
Phase 2.4 (7 pillars, 12 m, 3 m depth)	2,290	0,0056
Phase 2.5 (5 pillars, 20 m, 3 m depth)	1,970	0,0048
Phase 2.6 (5 pillars, 20 m, 1 m depth)	1,721	0,0042
Phase 2.7 (5 pillars, 20 m, 5 m depth)	1,821	0,0044
Phase 3.1 (multiple roads, 20 m, 10 m depth)	1,442	0,0035

As mentioned before, the CFD simulations were performed mainly to determine trends and to compare different situations that are normally difficult to simulate or even establish underground. From the information gathered, it should be possible to make more educated decisions on the layout of ventilation districts, the positioning of walls, the size of pillars, the effect of round and sharp edge pillars and the supply of air into sections and districts.

To simplify the use of all the relevant information by the ventilation practitioner, a summary is provided that could be used for a quick reference.

5.1   Summary of information for easy reference

The reader is urged to study this document carefully to obtain a complete picture of the vast amount of information that is available in this paper. Special attention should be given to the work published from overseas and also the results that were obtained from the CFD simulations. The information in this document will enlarge the general perspective of the behaviour of underground airflow as well as factors that might be considered when ventilation planning is executed. However, for the ventilation practitioner to be able to use the general values needed for simulations or problem solving exercises, the following tabulations are giving the most applicable values with regard to friction values for various coal mine underground situations:

Table 5.1:   Summary of applicable k-factor values for easy reference

K-FACTORS FOR CONVENTIONAL BORD AND PILLAR MINING	
LOW SEAM MINING (<2,0 metres)	Ns^2/m^4
Intake Airways	0,01107
Return Airways	0,01210
MEDIUM SEAM MINING (2,0 metres to 4,0 metres)	Ns^2/m^4
Intake Airways	0,01334
Return Airways	0,01467
HIGH SEAM MINING (>4,0 metres)	Ns^2/m^4
Intake Airways	0,01482
Return Airways	0,01584

K-FACTORS FOR MECHANICAL BORD AND PILLAR MINING	
LOW SEAM MINING (<2,0 metres)	Ns^2/m^4
Intake Airways	0,0095
Return Airways	0,0104
MEDIUM SEAM MINING (2,0 metres to 4,0 metres)	Ns^2/m^4
Intake Airways	0,0099
Return Airways	0,0109
HIGH SEAM MINING (>4,0 metres)	Ns^2/m^4
Intake Airways	0,0106
Return Airways	0,0117
K-FACTORS FOR DYKE EXCAVATION	Ns^2/m^4
K-factor for a typical dyke excavation	0,0854
K-FACTORS FOR VERTICAL SHAFTS	Ns^2/m^4
Concrete lines-no steelwork	0,004
Smooth lined, unobstructed	0,0037
Brick lined, unobstructed	0,0037
Brick lined, with rope guides and water and air ranges	0,0074
Concrete lined, with streamlined buntons	0,0045-0,025
Tubbing lined shaft with no guides or cages	0,0139
Brick lined shaft with two sets of side buntons	0,0176
Timber lined shaft with a middle line of buntons	0,0223
Concrete lined, with RSJ buntons	0,0075-0,060
Timbered rectangular	0,045-0,09
Heavily timbered rectangular	0,08
Empty raise-bore shaft	0,00731
INCLINE SHAFT K-FACTOR VALUES	Ns^2/m^4
Shafts for coal conveying and travelling	0,00947
Shafts for coal conveying only	0,00741
Shafts for travelling only	0,00674

RESISTANCE VALUES FOR AIRCROSSINGS	
INTAKE AIR SIDE	Ns^2/m^8
Resistance value per one aircrossing	0,00128
Resistance values per two aircrossings	0,00256
Resistance values per three aircrossings	0,00512
Resistance values per four aircrossings	0,00528
Resistance values per five aircrossings	0,00640
RETURN AIR SIDE	Ns^2/m^8
Resistance value per one aircrossing	0,00352
Resistance values per two aircrossings	0,00704
Resistance values per three aircrossings	0,01056
Resistance values per four aircrossings	0,01408
Resistance values per five aircrossings	0,01760

Regarding the shock losses as a result of pillar corners, the reader is referred back to the section 4.2.3 where the different pillar lengths has been simulated and a pressure loss per pillar has been calculated for a specific set of conditions. From the CFD results it was possible to determine a number that can be used to calculate the pressure loss that each pillar is causing. This value is to be used for planning purposes only as it was determined for an average set of conditions that would be generic for the coal mining industry. The value was determined for a side road depth of 3 metres, a roadway width of 6,6 metres and a seam height of 3,7 metres and the corners of the pillars were rounded. Further unofficial experiments has shown that these conditions provides the highest pressure loss per pillar and can therefore safely be used for planning purposes as any deviation from these set parameters could only improve the total pressure loss. Although the calculations were done for a single road situation, the simulations that were performed under phase 3, has shown that the number of roads does not indicate an increase in pressure loss. This means that the value below can be used for any number of roads that will be developed.

The value for calculating the pressure per pillar has been determined as:

$$\Delta P_{side\ roads} = 0,2147432.N$$

where N is the number of side roads. This gives the average pressure loss of **0,215 Pa** per 6,6 metre side road developed to 3 metre depth.

6 References Cited by Rahim et al[11]

[A] Clive, D. Hay, and I. C. F. Statham, "Mine Ventilation, A Review of Present Theory and Practice," {iTrans. Inst. Min. Engrs.}, vol. XCVIII, pp. 20-56, 1939.

[B] C. B. Jeppe, "Gold Mining on the Witwatersrand," {iTransvaal Chamber of Mines}, vol. 2, p. 1, 1946.

[C] W. E. Cooke and I. C. F. Stratham, "The Resistance to Airflow in Bends and Straight Airways," {iLoc-Cit}, vol. 6th Report of the Midland Institute on Ventilation of Mines, p. 188, 1928.

[D] G. B. Misra, {Mine Ventilation}. : Thaker Spink & Co., 1964.

[E] D. Murgue, "The friction of, or resistance to air currents in mines," {iTrans. Inst. of Min. Engrs}, vol. 6, pp. 135-176, 1893-94.

[F] G. E. McElroy and Richardson, {iFriction factors for metal airways}, usbm ri2663 ed. :, 1925.

[G] W. E. Cooke and I. C. F. Stratham, "Experiments on the Flow of Air in Ducts," {iLoc-Cit}, vol. 5th Report of the Midland Institute on Ventilation of Mines, p. 78, 1926.

[H] Anon., {iEstimating Ventilation Pressure in Mine Airways}, NCB Bulletin 53/73 ed. London: National Coal Board, 1953.

[I] A. Skochinsky and V. Komarov, {iMine Ventilation}. Moscow: Mir Publishers, 1969.

[J] S. Vujec, "Determination of Resistance in Mine Airways," {iRudarsko-Metalurski Zbornik}, vol. 1, pp. 71-83, 1970.

[K] J. R. Hodkinson, "Some Observations on the Law of Ariflow Resistance," {iColliery Engineer}, vol. XXXVI, p. 526, 1959.

[L] R. Clive, "The Comparative Resistance of Ventilation of Mine Roadways, Including the Working Face," {iTrans. of the Inst. of Mining Engineers}, vol. XCV, p. 325, 1937.

[M] D. Hay and W. E. Cooke, "Underground Tests on the Flow of Air at Rockingham Colliery," {iLoc-Cit}, vol. 71, p. 337, 1925.

6.1 References

1   W. Holding, "Resistance, resistance units and metrication," {imvs}, vol. 23, p. 181, 1970.

2   M. J. McPherson, "The metrication and rationalization of mine ventilation calculations," {iThe mining engineer}, vol. 131, pp. 729-738, 1971.

3   L. F. Moody, "Friction factors for pipe flow," {iTransactions of the american society of mechanical engineering}, vol. 66, pp. 671-677, 1944.

4   J. Burrows, "Note for students: 'K - The friction factor of an airway," {imvs}, vol. 28, pp. 60-61, 1975.

5   A. M. Wala, "Studies of friction factors for kentucky's coal mines," {iProceedings of 5th US mine ventilation symposium}, pp. 675-684, 1991.

6   M. O. Rahim, N. K. Patnaik, and S. P. Banerjee, "Determination of the Frictional Coefficient of Mine Airways with Varied Lining and Support Systems," {iJournal of Mines, Metal, and Fuels}, pp. 222-229, 1976.

7   P. Deglon and R. Hemp, "An evaluation of parameters to be used in colliery ventilation planning," {imvs}, pp. 369-376, 1992.

8   M. J. Martinson, J. R. Larson, and J. W. Andrews, "Measurement of airway resistance factors in a green river trona mine," {i3rd mvs}, pp. 486-492, 1987.

9   G. E. McElroy and A. S. Richardson, "Resistance of metal mine airways," {iDepartment of commerce, bureau of mines, bulletin 261}, p. 145, 1927.

10   R. Kharkar, R. Stefanco, and R. V. Ramani, "Analysis of leakage and friction factors in coal mine ventilation systems," {iSpecial research report, No SR-99PA, coal research board, commonwealth of Pennsylvania}, pp. 1-73, 1973.

12   M. J. McPherson, "The resistance of mine airways," {imvs}, vol. 28, pp. 149-157, 1975.

13   M. J. McPherson, "An analysis of the resistance and airflow characteristics of mine shafts," {i4th International mine ventilation congress}, pp. 55-92, 1988.

14   J. C. Tien, "Shock losses around underground overcasts," {i3rd mvs}, pp. 573-582, 1987.

15   W L Le Roux. Le Roux's notes on mine environmental control, Fourth edition. Mine Ventilation Society of South Africa publication

16   Mine Ventilation Society of South Africa, 1982. Environmental Engineering in South African Mines.

17   Mine Ventilation Society of SouthAfrica, 1992. The mine ventilation practitioner's Data Book.

18   Meyer C F December 1991. The effect of different last through road air velocities on unventilated headings. COMRO Reference Report No 4/91